



THE UNIVERSITY *of* EDINBURGH

Edinburgh Research Explorer

Dynamic GABAergic afferent modulation of AgRP neurons

Citation for published version:

Garfield, AS, Shah, BP, Burgess, CR, Li, MM, Li, C, Steger, JS, Madara, JC, Campbell, JN, Kroeger, D, Scammell, TE, Tannous, BA, Myers, MG, Andermann, ML, Krashes, MJ & Lowell, BB 2016, 'Dynamic GABAergic afferent modulation of AgRP neurons' Nature Neuroscience. DOI: 10.1038/nn.4392

Digital Object Identifier (DOI):

[10.1038/nn.4392](https://doi.org/10.1038/nn.4392)

Link:

[Link to publication record in Edinburgh Research Explorer](#)

Document Version:

Peer reviewed version

Published In:

Nature Neuroscience

Publisher Rights Statement:

This is the author's peer-reviewed manuscript as accepted for publication.

General rights

Copyright for the publications made accessible via the Edinburgh Research Explorer is retained by the author(s) and / or other copyright owners and it is a condition of accessing these publications that users recognise and abide by the legal requirements associated with these rights.

Take down policy

The University of Edinburgh has made every reasonable effort to ensure that Edinburgh Research Explorer content complies with UK legislation. If you believe that the public display of this file breaches copyright please contact openaccess@ed.ac.uk providing details, and we will remove access to the work immediately and investigate your claim.



Dynamic GABAergic afferent modulation of AgRP neurons

Alastair S Garfield^{1,2,9,10}, Bhavik P Shah^{1,9,10}, Christian R Burgess^{1,10}, Monica M Li^{1,10}, Chia Li^{3,4}, Jennifer S Steger¹, Joseph C Madara¹, John N Campbell¹, Daniel Kroeger⁵, Thomas E Scammell⁵, Bakhos A Tannous⁶, Martin G Myers Jr^{7,8}, Mark L Andermann¹, Michael J Krashes^{3,4} and Bradford B Lowell¹

¹Division of Endocrinology, Diabetes and Metabolism, Department of Medicine, Beth Israel Deaconess Medical Center, Harvard Medical School, Boston, Massachusetts 02115, USA.

²Centre for Integrative Physiology, Hugh Robson Building, University of Edinburgh, Edinburgh, EH8 9XD, UK.

³Diabetes, Endocrinology and Obesity Branch, National Institute of Diabetes and Digestive and Kidney Diseases, National Institutes of Health, Bethesda, Maryland 20892, USA.

⁴National Institute on Drug Abuse, National Institutes of Health, Baltimore, Maryland 21224, USA.

⁵Department of Neurology, Beth Israel Deaconess Medical Center, Harvard Medical School, Boston, Massachusetts 02115, USA.

⁶Department of Neurology, Massachusetts General Hospital, Harvard Medical School, Charlestown, Massachusetts 02129, USA.

⁷Department of Internal Medicine, University of Michigan, Ann Arbor, MI, USA

⁸Department of Molecular and Integrative Physiology, University of Michigan, Ann Arbor, MI, USA

⁹Present address: Cardiovascular and Metabolic Diseases, Pfizer, 610 Main Street, Cambridge, MA 02139, USA.

¹⁰Equal contribution

Correspondence: BBL blowell@bidmc.harvard.edu; ASG alastair.garfield@pfizer.com; MJK michael.krashes@nih.gov; MLA manderma@bidmc.harvard.edu

Running title: AgRP GABAergic afferents

Disclosure summary: The authors have nothing to disclose.

39 Abstract

40 Agouti-related peptide (AgRP) neurons of the arcuate nucleus of the
41 hypothalamus (ARC) promote homeostatic feeding at times of caloric
42 insufficiency, yet they are rapidly suppressed by food-related sensory cues prior
43 to ingestion. Here we identify a highly selective inhibitory afferent to AgRP
44 neurons that serves as a neural determinant of this rapid modulation.
45 Specifically, GABAergic projections arising from the ventral compartment of the
46 dorsomedial nucleus of the hypothalamus (vDMH) contribute to the pre-
47 consummatory modulation of ARC^{AgRP} neurons. In a manner reciprocal to
48 ARC^{AgRP} neurons, ARC-projecting leptin receptor (LepR)-expressing GABAergic
49 DMH neurons exhibit rapid activation upon availability of food that additionally
50 reflects the relative value of the food. Thus, DMH^{LepR} neurons form part of the
51 sensory network that relays real-time information about the nature and
52 availability of food to dynamically modulate ARC^{AgRP} neuron activity and feeding
53 behavior.

54 The sensory processing of caloric deficiency is critical to prevent starvation and
55 ensure survival¹. The fidelity of such need detection and response enactment is
56 defined by an evolutionarily conserved homeostatic system that links the
57 detection of this deficiency with the instinctual drive to consume food. ARC^{AgRP}
58 neurons have been classically viewed as a first-order interoceptive population
59 fundamental for this counter-regulatory response²⁻⁴. Indeed, increasing ARC^{AgRP}
60 neuron activity with mounting energy deficit reflects caloric need⁵ and promotes
61 a hardwired anabolic program that drives feeding behaviour^{3,6}. Experimentally,
62 activation of ARC^{AgRP} neurons during times of caloric repletion engenders a state
63 of artificial hunger⁷ that promotes motivated food seeking^{3,6} and consumption^{2,3}.
64 Remarkably however, recent investigation of the endogenous activity of ARC^{AgRP}
65 neurons has revealed that while a high firing rate during times of caloric
66 depletion permits overall feeding behavior, these neurons exhibit a rapid and
67 robust decrease in activity, the onset of which is coincident with the
68 detection/expectation of available food, prior to consumption (and maintained
69 throughout the feeding bout)^{5,7,8}. At present the functional significance of this
70 pre-consummatory suppression remains uncertain, with numerous non-
71 exclusive hypotheses proposed⁹, including a) its role as a preparatory/predictive
72 signal of future satiety (that prevents over-consumption and primes the celiac
73 response for ingestion), b) its requirement for the transition from food seeking
74 behavior to food consumption and c) its purpose as a negative teaching signal
75 that facilitates a learning-based association between detected food items and
76 future relief from hunger (following food ingestion)⁷.

77

78 Notwithstanding this issue, the rapidity of the ARC^{AgRP} neuron response to the
79 detection of food strongly suggests that the input responsible is neuronal in
80 origin. As such, an important first step in understanding the nature and
81 significance of the poly-synaptic connections that link food-related sensory input
82 with this rapid modulatory event is the identification of the pre-synaptic
83 population(s) that directly regulate ARC^{AgRP} neuron activity at fast timescales.
84 Here we identify an inhibitory afferent arising from the dorsomedial nucleus of
85 the hypothalamus (DMH) that is sufficient to robustly inhibit ARC^{AgRP} neurons
86 and suppress homeostatic feeding. Identified by their expression of the leptin
87 receptor (LepR) and of prodynorphin (pDYN), these pre-synaptic GABAergic
88 DMH neurons exhibit rapid pre-consummatory activation upon detection of food,
89 in a manner reciprocal to ARC^{AgRP} neurons. We conclude that this population
90 plays an important role in sensory cue-mediated regulation of ARC^{AgRP} neuron
91 activity.

92

93 **Results**

94 **vDMH^{LepR} neurons are ARC^{AgRP} neuron inhibitory afferents**

95 GABAergic modulation of ARC melanocortin neurons is well established to play a
96 role in the regulation of energy homeostasis^{10,11}. Previous monosynaptic rabies

97 mapping¹² from genetically-defined ARC^{AgRP} neurons identified the ARC, DMH
98 and, to a much lesser extent, the lateral hypothalamus (LH) as potential anatomic
99 sources of pre-synaptic input^{13,14}. To validate these observations and determine
100 their valence we employed channelrhodopsin-assisted circuit mapping (CRACM).
101 Using a *Slc32a1(vGAT)-ires-Cre* mouse to selectively transduce putative pre-
102 synaptic GABAergic neurons, we recorded post-synaptic currents on ARC^{AgRP}
103 neurons (as demarked by an *Npy-GFP* transgene that labels all ARC^{AgRP}
104 neurons^{15,16}). All recorded ARC^{AgRP} neurons exhibited picrotoxin-sensitive light-
105 evoked inhibitory post-synaptic currents (IPSCs) arising from distal DMH^{vGAT}
106 neurons (25/25; Fig 1a, S1a) and local ARC^{vGAT} neurons (10/10; Supplementary
107 Fig. 1b, d), but not from LH^{vGAT} neurons (0/13; Supplementary Fig. 1c, e).
108 However, ARC-projecting DMH^{vGAT} and ARC^{vGAT} neurons were also synaptically
109 connected to counteracting satiety-promoting ARC pro-opiomelanocortin
110 (POMC) neurons (demarked by a *Pomc-hrGFP* transgene; Fig 1b, Supplementary
111 Fig. 1f, g), negating the utility of the *vGAT-ires-Cre* mouse as a selective marker of
112 inhibitory ARC^{AgRP} neuron afferents.

113

114 We subsequently identified the leptin receptor (labeled by a *Lepr-ires-Cre* mouse
115 line) as a marker of GABAergic DMH afferents to ARC^{AgRP} neurons. Specifically,
116 CRACM analysis demonstrated that 100% of ARC^{AgRP} neurons (31/31; Fig 1c),
117 but only 9% of ARC^{POMC} neurons recorded (4/45; Fig 1d) and 5% of all ARC^{non-}
118 ^{AgRP} neurons (1/20; Supplementary Fig. 1h), received monosynaptic inhibitory
119 input from DMH^{LepR} neurons (and no glutamatergic input). Furthermore, and
120 consistent with their dense axo-somatic innervation of ARC^{AgRP} cell bodies (Fig
121 1e), pulsed light-evoked GABA release from DMH^{LepR}→ARC terminals was
122 sufficient to robustly suppress ARC^{AgRP} neuron action potential firing (Fig 1f).
123 Contrasting this selectivity, ARC^{LepR} neurons engaged 100% of recorded ARC^{AgRP}
124 (10/10; Supplementary Fig. 1i) and ARC^{POMC} neurons (21/21; Supplementary
125 Fig. 1j-k), while LH^{LepR} neurons did not engage either population (Supplementary
126 Fig. 1l-m). Thus, GABAergic DMH^{LepR} neurons represent a highly preferential and
127 potent source of pre-synaptic inhibitory input to ARC^{AgRP} neurons.

128

129 As revealed by pSTAT3 immunoreactivity (IR) GABAergic leptin-responsive DMH
130 neurons were largely restricted to the ventral compartment (Supplementary Fig.
131 2a), while the glutamatergic sub-population was localized to the dorsal regions
132 (Supplementary Fig. 2b). Consistent with this and the GABAergic nature of
133 vDMH^{LepR}→ARC^{AgRP} neurons (Fig 1c), the majority of vDMH ARC^{AgRP} afferents are
134 leptin-responsive (71±1.6%, n=3; Supplementary Fig. 2c-d). Together, these data
135 suggest that the vDMH is the principle source of GABAergic DMH LepR-
136 expressing ARC^{AgRP} neuron afferents. In addition, although as a population
137 DMH^{LepR} neurons are widely ramifying (Supplementary Fig. 3a), the ARC-
138 projecting axons do not collateralize to send projections to other

139 neuroanatomical targets (Supplementary Fig. 3b-c), as demonstrated by rabies
140 collateral mapping¹⁷.

141

142 **vDMH^{LepR}→ARC neurons are sufficient to inhibit feeding**

143 Since direct inhibition of ARC^{AgRP} neurons suppresses food consumption^{3,18} we
144 anticipated that the *in vivo* activation of vDMH^{LepR}→ARC projections would
145 similarly reduce food intake during times of physiological hunger, thus
146 confirming behaviorally the inhibitory nature of the circuit. *In vivo* optogenetic
147 stimulation of vDMH^{LepR}→ARC terminals facilitated the functional isolation of
148 this non-collateralizing circuit from the broader DMH^{LepR} population (Fig 2a).
149 Photostimulation of ChR2-mCherry expressing vDMH^{LepR}→ARC efferents
150 (Supplementary Fig. 4a) prior to the initiation of consumption (10 min or 10
151 sec), using the same pulsed-light protocol that successfully silenced *ex vivo*
152 ARC^{AgRP} neuron firing (Fig 1f, Supplementary Fig. 4b), significantly decreased
153 (~88%) dark-cycle food intake (Fig 2b); this was not observed in
154 photostimulated GFP-controls (Supplementary Fig. 4c). Optogenetic activation
155 also attenuated hyper-motivated food consumption following an overnight fast
156 (Fig 2c), while cessation of photostimulation rapidly reestablished normal
157 refeeding behavior (Fig 2c dashed line, Video 1). Interestingly, photostimulation
158 of this circuit was also sufficient to halt food intake 10 seconds after the
159 initiation of consumption following an overnight fast (Fig 2d) or during the dark
160 cycle (Supplementary Fig. 4d). Photostimulation in the dark cycle
161 (Supplementary Fig. 4e) or light cycle (Supplementary Fig. 4f) revealed no overt
162 changes in locomotor activity. No changes in anxiety-like behaviors were evident
163 in an open-field paradigm (Supplementary Fig. 4g-i). Photostimulation in the
164 fasted state increased the time spent grooming to a level comparable to that
165 following food intake (Supplementary Fig. 4j), consistent with an induction of
166 satiety-like behavior¹⁹. Chemogenetic silencing of DMH^{LepR} neurons did not
167 increase light-cycle food consumption (Supplementary Fig. 5), indicating that
168 this population is not required for maintaining physiological satiety. Together
169 these data demonstrate that vDMH^{LepR}→ARC neurons are sufficient, but not
170 necessary, to robustly suppress homeostatic feeding through the inhibition of
171 ARC^{AgRP} neurons and the induction of artificial satiety.

172

173 **vDMH^{LepR}→ARC neurons are activated by food availability**

174 Given these functional observations, and the inhibitory capacity of the
175 DMH^{LepR}→ARC projections, we considered whether vDMH^{LepR} neurons
176 contribute to the rapid and transient modulation of ARC^{AgRP} neurons upon
177 sensory detection of food^{5,7,8}. We therefore employed *in vivo* fiber photometry to
178 study the endogenous calcium activity of populations of vDMH^{LepR} neurons
179 during food presentation. Virally-mediated cre-dependent expression of the
180 genetically-encoded calcium indicator GCaMP6s²⁰ in vDMH^{LepR} neurons enabled
181 within-subject fluorometric analysis of real-time neuronal activity.

182 We first assessed the population response of vDMH^{LepR} cell bodies (Fig 3a) to
183 repeated presentation of small chow pellets (14 mg). In food-restricted mice
184 (85% of free-feeding body weight) we observed a rapid and robust increase in
185 calcium activity upon pellet detection and approach (Fig 3b-d), as compared to a
186 similar sized non-food object. This effect preceded the initiation of consumption
187 (Fig 3e). The absence of a significant calcium response to a non-food item also
188 confirms that the observed effect was not due to a startle response. In the *ad*
189 *libitum* fed state, when mice were calorically replete, calcium responses to
190 presentation of these pellets were significantly attenuated as compared to the
191 food-restricted state (Fig 3c-d). No calcium responses to food or object
192 presentation were evident from vDMH^{LepR} neurons transduced with cre-
193 dependent GFP (Supplementary Fig. 6a-b) or in validated ‘misses’ (no GCaMP6s
194 expression in DMH; Supplementary Fig. 6c-d). Thus, vDMH^{LepR} neurons exhibit a
195 pre-consummatory response that is similar in nature but opposite in sign to
196 AgRP neurons⁸ - a decrease in activity upon food presentation the magnitude of
197 which correlates with the animal’s hunger state.

198

199 Larger chow pellets (500 mg) also elicited a calcium response that exhibited
200 energy-state dependence (Fig 3f-g), however this response was of greater
201 magnitude than that observed with small pellets (Fig 3h), suggesting that
202 vDMH^{LepR} neuron activity conveys information not only about the presence but
203 the nature of discovered food items. ARC^{AgRP} neurons exhibit exaggerated pre-
204 consummatory suppression upon the presentation of chocolate - a highly
205 palatable food that is more calorically dense and rewarding (compared to
206 chow)⁸. As predicted, presentation of chocolate fragments (approximately 14
207 mg) elicited an increase in GCaMP6 fluorescence in DMH^{LepR} cell bodies. In
208 contrast to chow presentation, responses to chocolate presentation did not vary
209 across fasted vs. fed states (Fig 3i-j), possibly due to sustained food-seeking for
210 chocolate vs. chow pellets in the *ad libitum* fed state. Furthermore, and as
211 observed of ARC^{AgRP} neurons⁷, vDMH^{LepR} neuron fluorometric responses to
212 chocolate were significantly greater than to similar sized chow pellets (Fig 3k).
213 Thus, the pre-consummatory activation of vDMH^{LepR} neurons is potentiated by
214 the nutritive value of detected food, in a manner that reflects both food quantity
215 and quality.

216

217 To isolate the vDMH^{LepR}→ARC projecting neurons from the broader DMH^{LepR}
218 population, we assessed calcium activity specifically in vDMH^{LepR}→ARC axons
219 (Fig 4a). As observed in population activity from vDMH^{LepR} cell bodies, axonal
220 calcium activity in food-restricted mice rapidly increased upon small chow pellet
221 presentation (Fig 4b-d) prior to consumption (Fig 4e-g), but not in reaction to a
222 non-food object or in the *ad libitum* fed state. Larger chow pellets elicited larger
223 calcium responses compared to small pellets (Fig 4h and Supplementary Fig. 7a-
224 b), similar to responses in vDMH^{LepR} cell bodies. The vDMH^{LepR}→ARC axon

225 responses were larger to presentation of chocolate vs. small pellets, and did not
226 depend on hunger state (Fig 4i and Supplementary Fig. 7c-d). In sum,
227 vDMH^{LepR}→ARC neurons respond to availability of food in a manner opposite to
228 that of ARC^{AgRP} neurons, relaying real-time sensory information regarding the
229 availability and quality of food.

230

231 **A subset of vDMH^{LepR}→ARC neurons are dynorphinergic**

232 In light of the heterogeneity of DMH^{LepR} neurons²¹⁻²³, we sought to further
233 specify the neurochemical identity of GABAergic vDMH^{LepR}→ARC^{AgRP} afferents.
234 Recent analysis of hypothalamic LepR neurons has indicated that a subset of
235 those in the DMH express the inhibitory neuropeptide pDYN²⁴. Quantitative PCR
236 analysis of individual manually-isolated vDMH^{LepR} neurons revealed that 14/25
237 (56%) of those expressing *Slc32a1* (*vGAT*) also expressed *Pdyn* (Supplementary
238 Fig. 8a-b). Consistent with the location of vDMH^{LepR}→ARC^{AgRP} neurons
239 (Supplementary Fig. 2) the preponderance of leptin-responsive vDMH^{pDYN}
240 neurons (as defined by pSTAT3 immunoreactivity) were within the vDMH
241 (Supplementary Fig. 8c-e and Ref 18). Furthermore, projection profiling from
242 DMH^{pDYN} neurons identified the mediobasal ARC as their only long-range target
243 (Supplementary Fig. 8f-h).

244

245 CRACM analysis demonstrated that almost all recorded ARC^{AgRP} neurons (20/21;
246 Fig 5a) but no ARC^{non-AgRP} neurons (Supplementary Fig. 8i; including ARC^{POMC}
247 neurons, Fig 5b) received direct GABAergic input from vDMH^{pDYN} neurons.
248 vDMH^{pDYN}→ARC^{AgRP} IPSCs were of smaller amplitude compared to those derived
249 from vDMH^{LepR} afferents (Supplementary Fig. 8j) which led to less effective light-
250 evoked inhibition of ARC^{AgRP} neuron spiking (Supplementary Fig. 8k). This
251 suggests that vDMH^{pDYN} neurons are only a proportion of the total GABAergic
252 vDMH^{LepR}→ARC^{AgRP} population. *In vivo* optogenetic activation of vDMH^{pDYN}→ARC
253 terminals suppressed food consumption during the dark cycle (Fig 5c) and
254 following an overnight fast (Fig 5d). The magnitude of feeding suppression was
255 less than that observed of the vDMH^{LepR}→ARC circuit (Fig 2), especially during a
256 post-fast refeed, likely reflecting the weaker inhibitory potency of this circuit.

257

258 Subsequent *in vivo* GCaMP6s photometry demonstrated that vDMH^{pDYN} neurons
259 showed similar functional properties to vDMH^{LepR} neurons and DMH^{LepR}→ARC
260 axons. Small pellets presented to hungry mice elicited a significant increase in
261 calcium activity, prior to consumption, which was not observed upon detection
262 of a non-food item or in *ad libitum* fed mice (Fig 5e-g). Calcium responses in
263 food-restricted mice were potentiated by presentation of larger chow pellets (Fig
264 5h-j) and chocolate (Fig 5k-m), with chocolate responses being independent of
265 energy-state. Together, these data suggest that vDMH^{pDYN} neurons represent a
266 sub-population of GABAergic vDMH^{LepR}→ARC^{AgRP} afferents.

267

268 Discussion

269 Using a combination of *in vivo* techniques for the manipulation and monitoring of
270 genetically-defined neuronal populations we identify a source of inhibitory input
271 to ARC^{AgRP} neurons that contributes to their rapid sensory regulation^{5,7,8}. This
272 population of GABAergic vDMH^{LepR}/vDMH^{pDYN} neurons exhibits a highly
273 circumscribed efferent field within the ventromedial ARC with dense peri-
274 somatic innervation of ARC^{AgRP} somata. As such, they provide a highly selective
275 inhibitory input sufficient to robustly silence ARC^{AgRP} neuron action potential
276 firing and suppress homeostatic feeding, when photostimulated. It is important to
277 note that the complete inhibition of ARC^{AgRP} neurons by way of the optogenetic
278 activation of GABAergic vDMH^{LepR}→ARC terminals (Fig 1f) represents a supra-
279 physiological paradigm that exceeds the level of suppression induced by food
280 availability⁵. Thus, while providing behavioural validation for the nature of the
281 circuit such optogenetic manipulation does not speak to the physiological role of
282 ARC^{AgRP} neurons (or vDMH^{LepR}→ARC neurons) in the regulation of homeostatic
283 feeding. Indeed, as observed by others^{22,23}, DMH^{LepR} neurons were not necessary
284 for the maintenance of homeostatic satiety, indicating that they are not a source
285 of tonic ARC^{AgRP} neuron inhibition contributing to feeding suppression during
286 times of caloric sufficiency. This circuit may however offer a highly tractable
287 experimental approach for the real-time temporal control of ARC^{AgRP} neurons.

288
289 Recent investigations of the endogenous activity of ARC^{AgRP} neurons has revealed
290 their pre-consummatory suppression upon food presentation/expectation^{5,7,8}.
291 The rapidity of this response strongly suggests that it is synaptically, rather than
292 hormonally, mediated. Indeed, that all ARC^{AgRP} neurons recorded received
293 GABAergic vDMH^{LepR/pDYN} input is consistent with the majority of ARC^{AgRP}
294 neurons exhibiting pre-consummatory suppression^{5,7}. Thus, in light of the
295 specificity and potency of the vDMH^{LepR}→ARC circuit we asked whether it
296 contributed to the dynamic modulation of ARC^{AgRP} neurons during food
297 discovery. Strikingly, reciprocal to ARC^{AgRP} neurons, vDMH^{LepR} cell bodies and
298 vDMH^{LepR}→ARC axons exhibited rapid and reproducible pre-consummatory
299 activation upon food detection. Chow presentation elicited fluorescent responses
300 with both cue- and energy state-dependency, indicating some level of neural
301 gating upstream of these neurons is important for attributing salience to the
302 sensory input, in a manner that considers the animal's broader external and
303 internal environment. Furthermore, as observed of ARC^{AgRP} neurons⁸, the
304 magnitude of calcium responses in vDMH^{LepR} neurons and their ARC projections
305 increased with presentation of more palatable food. Thus, in the fasted state, the
306 potentiation of the vDMH^{LepR}→ARC response to increased nutritive content
307 (both quality and quantity) may signal the greater value of the food item as a
308 source of relief from hunger. However, as reflected by vDMH^{LepR}→ARC neuron
309 activity (and feeding behavior), food quantity loses, but food quality retains
310 incentive value in the calorically replete state, possibly suggesting a switch in

311 value processing from the homeostatic to the hedonic in the absence of a
312 physiological hunger drive.

313

314 Other populations of neuronal afferents also contribute to the sensory regulation
315 of ARC^{AgRP} neurons. Indeed, although vDMH^{LepR} neuron activity peaked upon
316 food approach prior to consumption, we observed a decay in the peak amplitude
317 of the calcium response before the termination of feeding. This contrasts with
318 the sustained reduction in ARC^{AgRP} neuron activity throughout consumption^{5,7,8}
319 and may suggest that additional inputs are important for prolonged ARC^{AgRP}
320 neuron suppression. This could include inhibition via other GABAergic afferents,
321 such as ARC^{vGAT} neurons, and/or dis-facilitation via removal of tonic excitatory
322 inputs – such as those arising from the PVH¹³. To this latter possibility, it is
323 interesting to note that ARC^{AgRP} neurons do not express the kappa-opioid
324 receptor (KOR)²⁵ (and data not shown), raising the possibility that any DYN
325 released from vDMH^{LepR/pDYN} neurons may act pre-synaptically to inhibit a KOR-
326 expressing excitatory ARC^{AgRP} neuron afferents. The kinetics of pre-synaptic
327 neuropeptide action would define a slower onset but longer-lasting modulation
328 of ARC^{AgRP} neurons and potentially explain their sustained suppression during
329 consumption. This model is also consistent with slow recovery in ARC^{AgRP}
330 neuron activity when presented food is subsequently removed prior to or during
331 the consummatory phase^{7,8}.

332

333 The significance of LepR expression on GABAergic vDMH^{LepR/pDYN}→ARC neurons
334 also remains to be determined. In acute electrophysiological slices leptin
335 depolarizes GABAergic vDMH^{LepR} neurons (data not shown). This raises the
336 possibility that low leptin levels, by decreasing the basal activity of these
337 neurons, may increase their dynamic range and facilitate their response to food
338 related sensory cues. Alternatively, it is possible that LepR signaling at these
339 neurons is involved in a slower transcriptional modulation, potentially related to
340 synaptic restructuring. In this way, LepR signaling at vDMH^{LepR}→ARC^{AgRP}
341 neurons may concern longer-term regulation reflecting the chronic nutritional
342 state, such as might underlie maladapted associations between sensory cues and
343 feeding behavior in obesity or eating disorders. Real-time monitoring of
344 vDMH^{LepR} neuron activity in diet-induced or genetically obese mice will prove
345 informative in this regard.

346

347 As a population, DMH^{LepR} neurons have been implicated in a number of
348 physiologies, including autonomic regulation of energy expenditure and
349 cardiovascular tone^{22,23,21}. Although the specific networks underlying these
350 functions are yet to be defined, it is likely that they are independent of the
351 vDMH^{LepR}→ARC^{AgRP} circuit. DMH^{LepR} neurons that regulate energy expenditure
352 are glutamatergic and located in the dorsal DMH^{22,26} and thus spatially and
353 neurochemically distinct from GABAergic vDMH^{LepR}→ARC^{AgRP} neurons.

354 Furthermore, the thermogenic effect of DMH^{LepR} neurons has been demonstrated
355 to be melanocortin independent²¹. For a number of reasons it is also unlikely
356 that the vDMH^{LepR}→ARC^{AgRP} circuit is involved in cardiovascular control. Firstly,
357 DMH mediated regulation of blood pressure is predicted to proceed via more
358 direct projections to pre-autonomic neurons in the RVLM²⁷. Secondly, leptin-
359 mediated or chemogenetic activation of DMH^{LepR} neurons only influences blood
360 pressure after 3 days of chronic simulation^{23,28}, inconsistent with the acute
361 modulatory function of vDMH^{LepR}→ARC^{AgRP} neurons. Thirdly, no feeding
362 suppression was observed during chemogenetically-induced hypotension²³, as
363 would be expected of activation of the vDMH^{LepR}→ARC^{AgRP} circuit. It is therefore
364 likely that vDMH^{LepR}→ARC neurons represent a functionally specific sub-
365 population involved in transitory sensory modulation of ARC^{AgRP} neurons. Of
366 note, LepR-expressing vDMH^{pDYN} neurons are distinct from the non-LepR
367 expressing cDMH^{pDYN} neurons implicated in the attenuation of food consumption
368 during intense feeding bouts²⁹.

369

370 The rapid pre-consummatory inhibition of ARC^{AgRP} neurons and their sustained
371 suppression during consumption represents a fascinating new aspect of their
372 physiological function^{5,7,8}, although the significance of this phenomenon for
373 feeding behaviour remains controversial. Our data now expand an
374 understanding of the nature and source of this modulation. Specifically, we
375 identify GABAergic vDMH^{LepR/pDYN} neurons as a potent inhibitory afferent to
376 ARC^{AgRP} neurons that, like their post-synaptic target, are rapidly regulated by
377 food detection. As expected, the directionality of this modulation is reciprocal to
378 ARC^{AgRP} neurons but occurs on a comparable timescale. Furthermore, like
379 ARC^{AgRP} neurons, vDMH^{LepR/pDYN} neuron activity reflects not only the presence,
380 but also the quality of the food item. These observations strongly support the
381 hypothesis that vDMH^{LepR/pDYN} neurons are a physiologically relevant source of
382 inhibitory input to ARC^{AgRP} neurons and provide an entry point into the
383 upstream circuitry that underlies rapid evaluation of sensory food cues during
384 homeostatic feeding.

385

386 **Acknowledgements**

387 This work was supported by the University of Edinburgh Chancellor's Fellowship
388 (ASG); National Institutes of Health: R01 DK096010 (BBL), R01 DK089044
389 (BBL), R01 DK071051 (BBL), R01 DK075632 (BBL), R37 DK053477 (BBL),
390 BNORC Transgenic Core P30 DK046200 (BBL), R01 DK056731 (MJG), BADERC
391 Transgenic Core P30 DK057521 (BBL); F32 DK089710 (MJK); DP2 DK105570-
392 01 (MLA), R01 DK109930 (MLA), the McKnight Foundation, the Klarman Family
393 Foundation (MLA), the Richard and Susan Smith Family Foundation (MLA) and
394 the Pew Scholars Program in Biomedical Sciences (MLA); ADA Mentor-Based
395 Fellowship (BPS and BBL); Davis Family Foundation postdoctoral fellowship
396 award (CRB); AHA postdoctoral fellowship (14POST20100011; JNC). This

397 research was supported, in part, by the Intramural Research Program of the NIH,
398 The National Institute of Diabetes and Digestive and Kidney Diseases (NIDDK;
399 DK075087, DK075088). GH Viral vector core facility funded by NIH/NINDS
400 (P30NS045776; BAT) for the preparation of the rabies virus. We thank Drs.
401 Jayaraman, Kerr, Kim, Looger, and Svoboda and the GENIE Project at Janelia
402 Farm Research Campus, Howard Hughes Medical Institute for distribution of
403 GCaMP6. We thank B. Sabatini and K. Wui Huang for assistance with *in vivo* fiber
404 photometry.

405

406 **Author contribution**

407 ASG, BPS, MJK and BBL conceived the studies. ASG, BPS, CRB, MML and MJK
408 conducted the studies with assistance from CL, JSS, JCM, DK and BAT.
409 Photometry experiments and analysis were conducted by CRB, MML and MLA.
410 Single cell qPCR analysis was conducted by JNC. ASG and BBL wrote the
411 manuscript with assistance from MGM and TES.

412

413 **References**

- 414 1. Sternson, S.M., Nicholas Betley, J. & Cao, Z.F. Neural circuits and
415 motivational processes for hunger. *Curr Opin Neurobiol* **23**, 353-360 (2013).
- 416 2. Aponte, Y., Atasoy, D. & Sternson, S.M. AGRP neurons are sufficient to
417 orchestrate feeding behavior rapidly and without training. *Nat Neurosci* **14**, 351-
418 355 (2011).
- 419 3. Krashes, M.J., *et al.* Rapid, reversible activation of AgRP neurons drives
420 feeding behavior in mice. *J Clin Invest* **121**, 1424-1428 (2011).
- 421 4. Luquet, S., Perez, F.A., Hnasko, T.S. & Palmiter, R.D. NPY/AgRP neurons
422 are essential for feeding in adult mice but can be ablated in neonates. *Science*
423 **310**, 683-685 (2005).
- 424 5. Mandelblat-Cerf, Y., *et al.* Arcuate hypothalamic AgRP and putative POMC
425 neurons show opposite changes in spiking across multiple timescales. *Elife* **4**
426 (2015).
- 427 6. Dietrich, M.O., Zimmer, M.R., Bober, J. & Horvath, T.L. Hypothalamic Agrp
428 neurons drive stereotypic behaviors beyond feeding. *Cell* **160**, 1222-1232
429 (2015).
- 430 7. Betley, J.N., *et al.* Neurons for hunger and thirst transmit a negative-
431 valence teaching signal. *Nature* **521**, 180-185 (2015).
- 432 8. Chen, Y., Lin, Y.C., Kuo, T.W. & Knight, Z.A. Sensory detection of food
433 rapidly modulates arcuate feeding circuits. *Cell* **160**, 829-841 (2015).
- 434 9. Chen, Y. & Knight, Z.A. Making sense of the sensory regulation of hunger
435 neurons. *Bioessays* **38**, 316-324 (2016).
- 436 10. Pinto, S., *et al.* Rapid rewiring of arcuate nucleus feeding circuits by leptin.
437 *Science* **304**, 110-115 (2004).
- 438 11. Vong, L., *et al.* Leptin action on GABAergic neurons prevents obesity and
439 reduces inhibitory tone to POMC neurons. *Neuron* **71**, 142-154 (2011).
- 440 12. Wickersham, I.R., Finke, S., Conzelmann, K.K. & Callaway, E.M. Retrograde
441 neuronal tracing with a deletion-mutant rabies virus. *Nat Methods* **4**, 47-49
442 (2007).

- 443 13. Krashes, M.J., *et al.* An excitatory paraventricular nucleus to AgRP neuron
444 circuit that drives hunger. *Nature* **507**, 238-242 (2014).
- 445 14. Wang, D., *et al.* Whole-brain mapping of the direct inputs and axonal
446 projections of POMC and AgRP neurons. *Front Neuroanat* **9**, 40 (2015).
- 447 15. van den Pol, A.N., *et al.* Neuromedin B and gastrin-releasing peptide excite
448 arcuate nucleus neuropeptide Y neurons in a novel transgenic mouse expressing
449 strong Renilla green fluorescent protein in NPY neurons. *J Neurosci* **29**, 4622-
450 4639 (2009).
- 451 16. Hahn, T.M., Breininger, J.F., Baskin, D.G. & Schwartz, M.W. Coexpression of
452 *Agrp* and NPY in fasting-activated hypothalamic neurons. *Nat Neurosci* **1**, 271-
453 272 (1998).
- 454 17. Betley, J.N., Cao, Z.F., Ritola, K.D. & Sternson, S.M. Parallel, redundant
455 circuit organization for homeostatic control of feeding behavior. *Cell* **155**, 1337-
456 1350 (2013).
- 457 18. Vardy, E., *et al.* A New DREADD Facilitates the Multiplexed Chemogenetic
458 Interrogation of Behavior. *Neuron* **86**, 936-946 (2015).
- 459 19. Rodgers, R.J., Holch, P. & Tallett, A.J. Behavioural satiety sequence (BSS):
460 separating wheat from chaff in the behavioural pharmacology of appetite.
461 *Pharmacol Biochem Behav* **97**, 3-14 (2010).
- 462 20. Chen, T.W., *et al.* Ultrasensitive fluorescent proteins for imaging neuronal
463 activity. *Nature* **499**, 295-300 (2013).
- 464 21. Enriori, P.J., Sinnayah, P., Simonds, S.E., Garcia Rudaz, C. & Cowley, M.A.
465 Leptin action in the dorsomedial hypothalamus increases sympathetic tone to
466 brown adipose tissue in spite of systemic leptin resistance. *J Neurosci* **31**, 12189-
467 12197 (2011).
- 468 22. Rezai-Zadeh, K., *et al.* Leptin receptor neurons in the dorsomedial
469 hypothalamus are key regulators of energy expenditure and body weight, but not
470 food intake. *Mol Metab* **3**, 681-693 (2014).
- 471 23. Simonds, S.E., *et al.* Leptin mediates the increase in blood pressure
472 associated with obesity. *Cell* **159**, 1404-1416 (2014).
- 473 24. Allison, M.B., *et al.* TRAP-seq defines markers for novel populations of
474 hypothalamic and brainstem LepRb neurons. *Mol Metab* **4**, 299-309 (2015).
- 475 25. Henry, F.E., Sugino, K., Tozer, A., Branco, T. & Sternson, S.M. Cell type-
476 specific transcriptomics of hypothalamic energy-sensing neuron responses to
477 weight-loss. *Elife* **4** (2015).
- 478 26. Knight, Z.A., *et al.* Molecular profiling of activated neurons by
479 phosphorylated ribosome capture. *Cell* **151**, 1126-1137 (2012).
- 480 27. Cao, W.H. & Morrison, S.F. Glutamate receptors in the raphe pallidus
481 mediate brown adipose tissue thermogenesis evoked by activation of
482 dorsomedial hypothalamic neurons. *Neuropharmacology* **51**, 426-437 (2006).
- 483 28. Fontes, M.A., Tagawa, T., Polson, J.W., Cavanagh, S.J. & Dampney, R.A.
484 Descending pathways mediating cardiovascular response from dorsomedial
485 hypothalamic nucleus. *Am J Physiol Heart Circ Physiol* **280**, H2891-2901 (2001).
- 486 29. Shek, E.W., Brands, M.W. & Hall, J.E. Chronic leptin infusion increases
487 arterial pressure. *Hypertension* **31**, 409-414 (1998).

488

489 **Figure legends:**

490

491 **Figure 1:**

492 **DMH^{LepR} neurons are a potent source of GABAergic input to ARC^{AgRP}**
 493 **neurons**
 494 **(a-b)**, DMH^{vGAT} neurons provide monosynaptic inhibitory input to 100% of
 495 ARC^{AgRP} neurons (a) and ARC^{POMC} neurons recorded (b). **(c-d)**, DMH^{LepR} neurons
 496 provide selective monosynaptic input to 100% of ARC^{AgRP} (c) but only 9% of
 497 ARC^{POMC} neurons recorded (d). **(e)**, DMH^{LepR}→ARC neurons provide dense axo-
 498 somatic innervation of ARC^{AgRP} neurons. **(f)**, Photostimulation of DMH^{LepR}→ARC
 499 terminals is sufficient to inhibit ARC^{AgRP} action potential firing. Abbreviations, 3v,
 500 third ventricle; PTX, picrotoxin. Scale bar in panel e, 100 μm and f, 25 μm.

501
 502 **Figure 2:**

503 **DMH^{LepR}→ARC neurons are sufficient to inhibit homeostatic feeding**

504 **(a-c)**, *in vivo* optogenetic stimulation of DMH^{LepR}→ARC terminals (a) significantly
 505 reduced food consumption during the dark-cycle (b; n=12, repeated measures
 506 ANOVA, main effect of treatment ($F_{(1,44)}=171.10$, $p<0.0001$), main effect of time
 507 ($F_{(3,44)}=48.48$, $p<0.0001$) and interaction ($F_{(3,44)}=30.95$, $p<0.0001$) and following
 508 an overnight fast (c; n=15, repeated measures ANOVA, main effect of treatment
 509 ($F_{(1,84)}=569.90$, $p<0.0001$), main effect of time ($F_{(3,84)}=226.50$, $p<0.0001$) and
 510 interaction ($F_{(3,84)}=43.74$, $p<0.0001$). **(d)**, photostimulation of DMH^{LepR}→ARC
 511 terminals in a post-fast refeed paradigm was sufficient to inhibit food intake
 512 when applied before or after food consumption had begun (n=7 (off) and 6 (on),
 513 ANOVA, $F_{(2,16)}=6.73$, $p=0.0074$). Abbreviations, Before, before food presentation;
 514 After, after the initiation of consumption. All data presented as mean±SEM; post-
 515 hoc p-values * $p<0.05$; *** $p<0.001$; **** $P<0.0001$.

516
 517 **Figure 3:**

518 **DMH^{LepR} neurons are rapidly activated upon sensory detection of food**

519 **(a)**, the real-time activity of DMH^{LepR} cell bodies was determined using *in vivo*
 520 fiber photometry. **(b-d)**, DMH^{LepR} neurons were rapidly activated upon
 521 presentation of a small chow pellet (t=0), compared to a non-food object, in a
 522 energy-state dependent manner (b, individual trials in one representative mouse
 523 on one day in the calorie restricted and *ad libitum* fed state; c, mean effects from
 524 all mice across time, n=6; d, mean response from 0-10s post food presentation,
 525 repeated measures ANOVA, $F_{(5,15)}=7.2$, $p=0.02$). **e**, responses of DMH^{LepR} to small
 526 pellet availability occurred prior to the initiation of consumption and was not
 527 increased further once consumption began (n=15; repeated measures ANOVA,
 528 $F_{(14,28)}=12.16$, $p=0.0002$). **(f-g)**, DMH^{LepR} neurons were rapidly activated upon
 529 presentation of a large chow pellet, compared to a non-food object, in a energy-
 530 state dependent manner (f, mean effects from all mice across time, n=6; d, mean
 531 response from 0-10s post food presentation, repeated measures ANOVA,
 532 $F_{(5,15)}=24.15$, $p=0.0001$). **(h)**, response of DMH^{LepR} neurons to large chow pellets
 533 was potentiated compared to that elicited by small chow pellets in the same
 534 mouse (n=7; paired t-test, $t_{(6)}=3.88$, $p=0.0081$). **(i-j)**, presentation of chocolate

535 activated DMH^{LepR} neurons, compared to a non-food object, and was comparable
 536 to responses in *ad libitum* chow-fed mice (i, mean effects from all mice across
 537 time, n=5; j, mean response from 0-10s post food presentation, repeated
 538 measures ANOVA, $F_{(4,12)}=24.21$, $p=0.0003$). (k), responses to chocolate were
 539 increased compared to chow (n=6, paired t-test, $t_{(5)}=4.58$, $p=0.006$). All data
 540 presented as mean \pm SEM; post-hoc p-values * $p<0.05$; ** $p<0.01$; **** $P<0.0001$.
 541 Abbreviations, $\Delta F/F$, fractional change in fluorescence.

542

543 **Figure 4:**544 **DMH^{LepR}→ARC axons are rapidly activated upon sensory detection of food**

545 (a), the real-time activity of DMH^{LepR}→ARC axons was determined using *in vivo*
 546 fiber photometry. (b-d), DMH^{LepR}→ARC axons were rapidly activated upon
 547 presentation of a small chow pellet (t=0), compared to a non-food object, in a
 548 energy-state dependent manner (b, individual trials in one representative mouse
 549 on one day in the calorie restricted and ad libitum fed state; c, mean effects from
 550 all mice across time, n=6; d, mean response from 0-10s post food presentation,
 551 repeated measures ANOVA, $F_{(5,15)}=36.08$, $p<0.0001$). (e), activation of
 552 DMH^{LepR}→ARC axons to small pellet availability occurred prior to the initiation
 553 of consumption (n=36; repeated measures ANOVA, $F_{(35,70)}=35.30$, $p<0.0001$). (f-
 554 g), Mean responses to small pellet presentation aligned to onset of consumption
 555 (f) and individual trial responses aligned to food availability (g; onset of
 556 consumption denoted with vertical black bar on each trial) demonstrating
 557 activity rising prior to consumption. (h-i), calcium response of DMH^{LepR}→ARC
 558 axons to large chow pellets (h; n=6; paired t-test, $t_{(6)}=3.61$, $p=0.015$) and
 559 chocolate (i; n=6; paired t-test, $t_{(6)}=3.13$, $p=0.026$) were potentiated compared to
 560 that elicited by small chow pellets in the same mouse. All data presented as
 561 mean \pm SEM; post-hoc p-values * $p<0.05$; ** $p<0.01$; *** $p<0.001$; **** $P<0.0001$.
 562 Abbreviations, $\Delta F/F$, fractional change in fluorescence.

563

564 **Figure 5:**565 **DMH^{pDYN} neurons are a subset of GABAergic DMH^{LepR}→ARC neurons**

566 (a-b), DMH^{pDYN} neurons (red) provide monosynaptic inhibitory input to 95% of
 567 ARC^{AgRP} (a; 20/21 connected) neurons recorded but not ARC^{POMC} neurons (b;
 568 0/12 connected). (c-d), *in vivo* optogenetic stimulation of DMH^{pDYN}→ARC
 569 terminals significantly reduced food consumption during the dark-cycle (c; n=3,
 570 repeated measures ANOVA, main effect of treatment ($F_{(1,8)}=77.14$, $p<0.0001$),
 571 main effect of time ($F_{(3,8)}=21.49$, $p=0.0003$) and interaction ($F_{(3,8)}=12.69$,
 572 $p=0.002$) and following an overnight fast (d; n=3, repeated measures ANOVA,
 573 main effect of treatment ($F_{(1,8)}=193.60$, $p<0.0001$), main effect of time
 574 ($F_{(3,8)}=111.90$, $p<0.0001$) and interaction ($F_{(3,8)}=22.63$, $p=0.0003$). (e-f), *in vivo*
 575 fiber photometry demonstrated that DMH^{pDYN} neurons were rapidly activated
 576 upon presentation of a small chow pellet (t=0), compared to a non-food object, in
 577 a energy-state dependent manner (e, mean effects from all mice across time,

578 n=5-6; f, mean response from 0-10s post food presentation, one-way ANOVA,
579 $F_{(3,18)}=19.56$, $p<0.0001$). (g), activation of DMH^{pDYN} to small pellet availability
580 occurred prior to the initiation of consumption and was not increased further
581 once consumption began (n=44; repeated measures ANOVA, $F_{(43,86)}=40.61$,
582 $p<0.0001$). (h-i), DMH^{pDYN} neurons were rapidly activated upon presentation of a
583 large chow pellet, compared to a non-food object, in a energy-state dependent
584 manner (h, mean effects from all mice across time, n=5-6; i, mean response from
585 0-10s post food presentation, one-way ANOVA, $F_{(3,18)}=13.43$, $p<0.0001$). (j),
586 calcium response of DMH^{pDYN} neurons to large chow pellets was potentiated
587 compared to that elicited by small chow pellets in the same mouse (n=6; paired
588 t-test, $t_{(5)}=3.56$, $p=0.016$). (k-l), presentation of chocolate activated DMH^{pDYN}
589 neurons, compared to a non-food object, and was comparable to *ad libitum*
590 chow-fed mice (k, mean effects from all mice across time, n=5-6; l, mean
591 response from 0-10s post food presentation, one-way ANOVA, $F_{(3,18)}=18.03$,
592 $p<0.0001$). (m), DMH^{pDYN} neuron calcium responses to chocolate were increased
593 compared to chow (n=6, paired t-test, $t_{(5)}=5.09$, $p=0.0038$). All data presented as
594 mean±SEM; post-hoc p-values: * $p<0.05$; ** $p<0.01$; *** $p<0.001$; **** $P<0.0001$.
595 Abbreviations, $\Delta F/F$, fractional change in fluorescence.

596

597

598 **Material and methods:**

599

600 **Animals**

601 *Slc32a1(vGAT)-ires-Cre¹¹*, *Lepr-ires-Cre³⁰*, *Pdyn-ires-Cre¹³*, *Npy-hrGFP¹⁵*, *Pomc-*
602 *hrGFP³¹*, *Rosa26-loxSTOPlox-L10-GFP¹³* mice were generated and maintained as
603 previously described. All mice are on a mixed background. All animal care and
604 experimental procedures were approved by the National Institute of Health and
605 Beth Israel Deaconess Medical Center Institutional Animal Care and Use
606 Committee. Mice were housed at 22–24 °C with a 12 h light:12 h dark cycle with
607 standard mouse chow (Teklad F6 Rodent Diet 8664; 4.05 kcal g⁻¹, 3.3 kcal g⁻¹
608 metabolizable energy, 12.5% kcal from fat; Harlan Teklad) and water provided
609 *ad libitum*, unless otherwise stated. All diets were provided as pellets. For all
610 behavioral studies male mice between 6-10 weeks were used. For
611 electrophysiological studies male mice between 4-8 weeks were used.

612

613 **Brain tissue preparation**

614 Mice were terminally anesthetised with chloral hydrate (Sigma Aldrich) and
615 transcardially perfused with phosphate-buffered saline (PBS) followed by 10%
616 neutral buffered formalin (Fisher Scientific). Brains were extracted,
617 cryoprotected in 20% sucrose, and sectioned coronally on a freezing sliding
618 microtome (Leica Biosystems) at 30 μm and collected in four equal series.

619

620 Immunohistochemistry

621 Brain sections were washed in 0.1 M phosphate-buffered saline pH 7.4, blocked
622 in 3% normal donkey serum/0.25% Triton X-100 in PBS for 1 hour at room
623 temperature and then incubated overnight at room temperature in blocking
624 solution containing primary antiserum (rabbit anti-dsRed, Clontech (#632496)
625 1:1000; chicken anti-GFP, Life Technologies (#A10262). The next morning
626 sections were extensively washed in PBS and then incubated in Alexa
627 fluorophore secondary antibody (Molecular Probes, 1:1000) for 2 h at room
628 temperature. After several washes in PBS, sections were mounted onto gelatin-
629 coated slides and fluorescent images were captured with Olympus VS120 slide
630 scanner microscope. All primary antibodies used are validated for species and
631 application (1DegreeBio and Antibody Registry).

632

633 pSTAT3 immunohistochemistry

634 Mice were injected with 5 mg/kg recombinant leptin two hours prior to
635 perfusion (as above). Brain sections were washed in 0.1 M phosphate-buffered
636 saline pH 7.4 followed by incubation in 5% NaOH and 0.3% H₂O₂ for 2 min, then
637 with 0.3% glycine (10 min), and finally with 0.03% SDS (10 min), all made up in
638 PBS. Sections were blocked in 3% normal donkey serum/0.25% Triton X-100 in
639 PBS for 1 hour at room temperature and then incubated overnight at room
640 temperature in blocking solution containing 1/250 rabbit anti-pSTAT3 (Cell
641 Signalling, #9145) and 1/1000 chicken anti-GFP (Life Technologies, #A10262).
642 The next morning sections were extensively washed in PBS and then incubated
643 in 1/250 donkey anti-rabbit 594 (Molecular Probes, R37119) and 1/1000
644 donkey anti-chicken 488 (Jackson ImmunoResearch, 703-545-155) for 2 h at
645 room temperature. After several washes in PBS, sections were mounted onto
646 gelatin-coated slides and fluorescent images were captured with Olympus VS120
647 slide scanner microscope.

648

649 Single cell quantitative PCR

650 DMH was acutely dissected from adult *LepR-ires-Cre::L10-GFP* mice (n=2), then
651 enzymatically dissociated and manually sorted for GFP+ cells as described
652 previously³². Isolated GFP positive cells and negative control samples (cell-
653 picking buffer) were concurrently processed into cDNA libraries using Smart-
654 Seq2³³, except that the amplified cDNA was eluted in 30 µl volumes. Gene
655 expression was analyzed by probe-based qPCR on a 7500 Fast Real-Time PCR
656 System (Applied Biosystems) using Brilliant II qPCR Low ROX Master Mix
657 (Agilent Technologies) according to the manufacturer's instructions. Each 20 µl
658 qPCR reaction contained 2 µl of eluted cDNA and 1 µl of a custom primer/probe
659 set (sequences below; 1:1 ratio of primer:probe; default FAM/ZEN modifications;
660 IDT). Cells showing relatively little to no expression of *Gfp*, *Actb*, or *Slc32a1* were
661 excluded from further analysis. Remaining cells were analyzed for expression of
662 *Pdyn*. A heatmap of Ct values was generated using GenePattern software (Broad

663 Institute), with a “global” color scale for across-gene comparisons. Note that in
664 order to include cells for which no signal was detected in 40 cycles of qPCR, a
665 “pseudocount” of 40 was entered as the Ct. Primers (5'→3'): *Actb* (L,
666 AAAAGGGAGGCTCAGACCTGG; R, TCACCCTCCAAAAGCCACC; probe,
667 GCCCTGAGTCCACCCCGGGG); *Gfp* (L, ATCTGCACCACCGGCAAGCT; R,
668 ATCTGCACCACCGGCAAGCT; probe, CGTGCCCTGGCCCACCCTCG); *Slc32a1* (L,
669 ACGAGCACACCACGCACA; R, ATTCGGGCGGGCGACTTCA; probe,
670 GGCCCCGTTTGCCTGCCGGT); *Pdyn* (L, AGGATGGGGATCAGGTAGGGCA; R,
671 CACCTTGAAGTACGCCGCA; probe, GGGGGCTTCTGCGGCGCAT).

672

673 ***Viral injections***

674 Stereotaxic injections were performed as previously described. Mice were
675 anaesthetised with xylazine (5 mg per kg) and ketamine (75 mg per kg) diluted
676 in saline (350 mg per kg) and placed into a stereotaxic apparatus (KOPF Model
677 963 or Stoelting). For postoperative care, mice were injected intraperitoneally
678 with meloxicam (5 mg/kg). After exposing the skull via small incision, a small
679 hole was drilled for injection. A pulled-glass pipette with 20–40 mm tip diameter
680 was inserted into the brain and virus was injected by an air pressure system. A
681 micromanipulator (Grass Technologies, Model S48 Stimulator) was used to
682 control injection speed at 25 nl min⁻¹ and the pipette was withdrawn 5 min after
683 injection. For electrophysiology and *in vivo* optogenetic experiments, AAV8-
684 hSyn-DIO-ChR2(H134R)-mCherry (University of North Carolina Vector Core;
685 titer 1.3 × 10¹² genome copies per ml) was injected into the ARC (15-50 nl, AP: –
686 1.50 mm, DV: –5.80 mm, ML: +/-0.20 mm from bregma), DMH (50 nl, AP: -1.80
687 mm, DV: -5.2 mm, ML: +/-0.3 mm from bregma), LH (50-100 nl, AP: –1.50 mm,
688 DV: –5.00 mm, ML: +/-1.00 mm from bregma). For electrophysiology and *in vivo*
689 chemogenetic experiments, AAV8-hSyn-DIO-hM4Di-mCherry (University of
690 North Carolina Vector Core; titer 1.7 × 10¹² genome copies per ml) were
691 bilaterally injected into the DMH (15-40 nl, coordinates as above). For *ex vivo*
692 and *in vivo* calcium imaging experiments, AAV1-hSyn-DIO-GCaMP6(s)
693 (University of Pennsylvania Vector Core) was injected into the DMH (50 nl,
694 coordinates as above). Mice were given a minimum of 2 weeks recovery and 1
695 week acclimation before being used in any experiments.

696

697 ***Electrophysiology***

698 To prepare brain slices for electrophysiological recordings, brains were removed
699 from anesthetized mice (4-8 weeks old) and immediately submerged in ice-cold,
700 carbogen-saturated (95% O₂, 5% CO₂) high sucrose solution (238 mM sucrose,
701 26 mM NaHCO₃, 2.5 mM KCl, 1.0 mM NaH₂PO₄, 5.0 mM MgCl₂, 10.0 mM CaCl₂,
702 11 mM glucose). Then, 300-μm thick coronal sections were cut with a Leica
703 VT1000S Vibratome and incubated in oxygenated aCSF (126 mM NaCl, 21.4 mM
704 NaHCO₃, 2.5 mM KCl, 1.2 mM NaH₂PO₄, 1.2 mM MgCl₂, 2.4 mM CaCl₂, 10 mM
705 glucose) at 34 °C for 30 min. Then, slices were maintained and recorded at room

706 temperature (20–24°C). For most voltage clamp recordings intracellular solution
 707 contained the following (in mM): 140 CsCl, 1 BAPTA, 10 HEPES, 5 MgCl₂, 5 Mg-
 708 ATP, 0.3 Na₂GTP, and 10 lidocaine *N-ethyl* bromide (QX-314), pH 7.35 and 290
 709 mOsm. The intracellular solution for current clamp recordings contained the
 710 following (in mM): 128 K gluconate, 10 KCl, 10 HEPES, 1 EGTA, 1 MgCl₂, 0.3
 711 CaCl₂, 5 Na₂ATP, 0.3 NaGTP, adjusted to pH 7.3 with KOH.

712 Light-evoked IPSCs and EPSCs during CRACM studies^{34,35} were recorded in the
 713 whole cell voltage clamp mode, with membrane potential clamped at -60 mV. In
 714 a subset of voltage clamp CRACM experiments it was necessary to detect light-
 715 evoked GABAergic synaptic currents in ChR2-mCherry expressing neurons
 716 (Supplementary Fig. 2d, h, i). As such, to negate the movement of monovalent
 717 cations, a Cs⁺ based low Cl⁻ internal solution was used (129 mM CsMeSO₄, 16 mM
 718 CsCl, 8mM NaCl, 10 mM HEPES, 0.25 mM EGTA, 3 mM Mg-ATP, 0.3 mM Na₂GTP)
 719 and light-evoked IPSCs recorded at ~0 mV. All recordings were made using
 720 multiclamp 700B amplifier, and data was filtered at 2 kHz and digitized at 10
 721 kHz. To photostimulate Channelrhodopsin2-positive fibers, a laser or LED light
 722 source (473 nm; Opto Engine LLC; Thorlabs) was used. The blue light was
 723 focused on to the back aperture of the microscope objective, producing a wide-
 724 field exposure around the recorded cell of 1 mW. The light power at the
 725 specimen was measured using an optical power meter PM100D (ThorLabs). The
 726 light output is controlled by a programmable pulse stimulator, Master-8 (AMPI
 727 Co. Israel) and the pClamp 10.2 software (AXON Instruments). Photostimulation-
 728 evoked EPSCs/IPSCs detection protocol constitutes four blue light laser pulses
 729 (pulse duration - 2 ms) administered 1 second apart, repeating for a total of 30
 730 sweeps. When recording light-evoked changes in membrane potential in AgRP
 731 neurons, current (~5 pA) was injected into cells to maintain continuous action
 732 potential firing.

733

734 Number of animals used per study (all male): DMH^{vGAT}→ARC^{AgRP} *n*=2;
 735 DMH^{vGAT}→ARC^{POMC} *n*=3; ARC^{vGAT}→ARC^{AgRP} *n*=4; ARC^{vGAT}→ARC^{POMC} *n*=5; LH^{vGAT}
 736 →ARC^{AgRP} *n*=2; LH^{vGAT}→ARC^{POMC} *n*=2; DMH^{LepR}→ARC^{AgRP} *n*=3;
 737 DMH^{LepR}→ARC^{POMC} *n*=6; ARC^{LepR}→ARC^{AgRP} *n*=2; ARC^{LepR}→ARC^{POMC} *n*=4; LH^{LepR}
 738 →ARC^{AgRP} *n*=1; LH^{LepR}→ARC^{POMC} *n*=3. DMH^{pDYN}→ARC^{AgRP} *n*=4;
 739 DMH^{pDYN}→ARC^{POMC} *n*=2.

740

741 **Optic fiber implantation**

742 Optic fiber implantations were performed during the same surgery as viral
 743 injection (above). For optogenetic photostimulation of DMH→ARC terminals,
 744 ceramic ferrule optical fibers (200 μm diameter core, BFH37-200 Multimode, NA
 745 0.37; Thor Labs) were implanted bilaterally over the ARC (AP: -1.55 mm, DV: (R)
 746 -5.75 mm and (L) - 5.50 mm, ML: (R) +0.3 mm and (L at 20°) -2.40 mm from
 747 bregma). For DMH^{LepR} and DMH^{pDYN} cell body calcium photometry a metal

748 ferrule optic fiber (200 μm diameter core; BFH37-200 Multimode; NA 0.37; Thor
749 Labs) was implanted unilaterally over the vDMH (AP: -1.80 mm, DV: -5.0 mm,
750 ML: +0.3 mm from bregma). For DMH^{LepR}→ARC axon calcium photometry a
751 metal ferrule optic fiber (400 μm diameter core; BFH37-400 Multimode; NA
752 0.37; Thor Labs) was implanted unilaterally over the ARC (AP: -1.55 mm, DV: -
753 5.8 mm, ML: (at 2°) -0.49 mm from bregma). Fibers were fixed to the skull using
754 dental acrylic and mice were allowed 2 weeks for recovery before
755 acclimatisation to home cages customized for optogenetic stimulation or
756 photometry recording (12 h light/dark cycle starting at 6am) for 1 week. After
757 the completion of the experiments, mice were perfused and the approximate
758 locations of fiber tips were identified based on the coordinates of Franklin and
759 Paxinos.³⁶

760

761 ***Food intake studies***

762 Food intake studies on chow were performed as previously described. All
763 animals were singly housed for at least 2.5 weeks following surgery and handled
764 for 10 consecutive days before the assay to reduce stress response. Studies were
765 conducted in a home-cage environment with *ad libitum* food access. A full trial
766 consisted of assessing food intake from the study subjects after they received
767 injections of saline or pseudo-photostimulation on day-1 and 1 mg/kg CNO or
768 photostimulation on day-2. Animals received a week 'off' between trials before
769 another trial was initiated. The food intake data from all days were then
770 averaged and combined for analysis. Mice with 'missed' injections, incomplete
771 'hits' or expression outside the area of interest were excluded from analysis after
772 post hoc examination of mCherry expression. In this way, all food intake
773 measurements were randomised and blind to the experimenter.

774

775 Dark-cycle feeding studies were conducted between 6:00pm to 9:00pm and
776 intake was monitored for three hours. For post-fast refeed studies, animals were
777 fasted overnight at 5:00pm and food returned the following morning at 9:00am.
778 Food intake was monitored for five hours after photostimulation. Light-cycle
779 feeding studies were conducted between 9:00am to 12:00pm and intake was
780 monitored for three hours.

781

782 ***In vivo optogenetic studies***

783 *In vivo* photostimulation was conducted as previously described³². Fiber optic
784 cables (1.25 m long, 200 μm diameter, 0.37 NA; Doric Lenses) were firmly
785 attached to the implanted fiber optic cannulae with zirconia sleeves (Doric
786 Lenses). Animals were stimulated with blue light (473 nm) at 10 Hz, 5 ms pulses
787 for 5 sec with a 1 sec recovery period (laser off) during stimulation trains to
788 avoid neuronal transmitter depletion and tissue heating. Photostimulation was
789 provided using a waveform generator (PCGU100; Valleman Instruments or
790 Arduino electronics platform) that provided TTL input to a blue light laser

791 (Laserglow). We adjusted the power of the laser such that the light power exiting
792 the fiber optic cable was at least 10 mW. Using an online light transmission
793 calculator for brain tissue [http://web.stanford.edu/group/dlab/cgi-](http://web.stanford.edu/group/dlab/cgi-bin/graph/chart.php)
794 [bin/graph/chart.php](http://web.stanford.edu/group/dlab/cgi-bin/graph/chart.php) we estimated the light power at the ARC to be 18.35
795 mW/mm². Mice were tethered to the patch cords at least 1 hour prior to the
796 commencement of any experiment.

797

798 To test the sufficiency of DMH^{LepR}→ARC neurons for satiety mice were tested
799 under two conditions of physiological hunger, at the onset of the dark cycle and
800 refeeding following an overnight fast.. For dark cycle feeding analysis mice with
801 *ad libitum* access to food were photostimulated for 10 min prior to the onset of
802 the dark cycle (which serves as a natural cue for the initiation of feeding
803 behaviour) and photostimulation maintained for the duration of the study. For
804 post-fast refeeding analysis mice were photostimulated 10 min prior to food
805 presentation (which serves as an experimental cue for the initiation of feeding
806 behaviour) and photostimulation maintained for the duration of the study. In
807 the explicit case of the 'ON (After) group' in Figure 2D, mice were allowed to
808 consume freely for 5 min and then photostimulated for the duration of the
809 experiment.

810

811 ***Behavioural profiling***

812 Open field testing was conducted in *ad libitum* fed mice during the light cycle.
813 Mice were placed in a large arena (40 cm x 40 cm) in which they were allowed to
814 freely explore for 20 min. Trials were recorded via a CCD camera interfaced with
815 Ethovision software for offline analysis of distance moved, time spent at the edge
816 and center of the arena. Animals were run in a counter-balanced order of laser-
817 on versus laser-off to avoid acclimation.

818

819 For assessment of homecage behaviour mice were compared in the fasted state
820 with photostimulation and *ad libitum* fed state during the light cycle in the
821 absence of food. 10 minute trials were recorded via a CCD camera interfaced
822 with Ethovision software for offline analysis of time spent grooming and total
823 distance moved. Animals were run in a counter-balanced order of laser-on
824 versus laser-off to avoid acclimation. Locomotor activity during the dark cycle
825 was also assessed in *ad libitum* fed mice with and without laser stimulation, in
826 the presence of food.

827

828 ***In vivo fiber photometry***

829 All photometry experiments were conducted as within-subject, with animals
830 tested in both the fed and fasted state. Studies were conducted in the animal's
831 homecage. Beginning two weeks post-surgery (details above) mice were food
832 restricted to 85-90% of starting body weight. Over this one week period mice
833 were acclimated to the chow pellets (both small and large) used in subsequent

834 photometry experiments. Mice were habituated to the paradigm for 1-2 days
835 prior to the first recording day. *In vivo* fiber photometry was conducted as
836 previously described⁸. Fiber optic cables (1 m long, metal ferrule, 400 μ m
837 diameter; Doric Lenses) were firmly attached to the implanted fiber optic
838 cannulae with zirconia sleeves (Doric Lenses). Laser light (473 nm) was focused
839 on the opposite end of the fiber optic cable such that a light intensity of 0.1-
840 0.2mW entered the brain; light intensity was kept constant across sessions for
841 each mouse. Emission light was passed through a dichroic mirror (Di02-R488-
842 25x36, Semrock) and GFP emission filter (FF03-525/50-25, Semrock), before
843 being focused onto a sensitive photodetector (2151, Newport). The signal was
844 passed through a low-pass filter (50Hz) and digitized with a National
845 Instruments data acquisition card and collected using a custom MATLAB script.
846 Photobleaching over the course of each 30 min run was negligible, most likely
847 due to the very low laser power used for excitation (0.1 mW) and the short
848 duration of each run. Although we continued to observe clear responses to food
849 presentation at the end of each run (in the food restricted state) we did note
850 average 37% decrease between first and last responses. It is possible that minor
851 photobleaching contributed to this effect, though it was likely predominantly due
852 to reduced novelty of food and some level of caloric repletion.

853

854

855 Each 30 minute session consisted of 4-6 trials of chow (14 mg pellets) or
856 chocolate (14 mg pellets) and 4-6 trials of a similar sized non-food object
857 (bedding), in an alternating fashion. Large pellets (500 mg) required up to 15
858 minutes to consume and therefore only had 1-2 presentations per a run, with
859 alternating non-food item presentation. Only one food type was used in a given
860 run. Up to 4 runs were performed in a single day for each mouse and mice were
861 run multiple days, with large pellet and chocolate runs never preceding small
862 pellet runs. All trials across days (14mg: 12 ± 1 presentations per mouse; 500
863 mg: 6 ± 0.7 ; chocolate: 7 ± 0.6) were pooled to calculate mean response to
864 food/object in each mouse. After fasted runs mice were given *ad libitum* access
865 to chow for 5-7 days and the above studies repeated in the fed state. Within run
866 responses to the same food stimulus showed a trend towards a decrease in
867 response magnitude (decreasing by 37% from the first to the last instance of
868 food availability; data not shown) this may reflect decreasing novelty or
869 increasing satiety (as mice had consumed food throughout the run prior to the
870 last instance of food presentation).

871

872 For data analysis, fluorescent traces were down-sampled to 1Hz. dF/F ($F -$
873 F_0)/ F_0 ; where F_0 was the 20 sec prior to food presentation) was calculated for
874 each presentation of food. Small pellets (per 14mg pellet 0.01 Kcal from protein,
875 0.007 Kcal from fat and 0.03 Kcal from carbohydrate; Bio-Serv). Large pellets
876 (per 500 mg pellet 0.38 Kcal from protein, 0.25 Kcal from fat and 1.18 Kcal from

877 carbohydrate; Bio-Serv) or 14 mg chocolate (Hershey's) or control (cob bedding
878 of size comparable to food). In a subset of mice both time of food availability
879 and the moment when the mouse first made contact with the food item were
880 recorded. For analysis differentiating approach from consumption, the 10s prior
881 to food availability was compared to the time between food availability and
882 consumption and to the 10s following contact with the food item.

883

884 ***Monosynaptic rabies mapping***

885 *AgRP-ires-Cre::RABVgp4-TVA* mice expressing the avian TVA receptor and rabies
886 glycoprotein selectively in ARC^{AgRP} neurons were injected with SADΔG-EGFP
887 (EnvA) rabies (Salk Gene Transfer Targeting and Therapeutics Core; titer 7.5 x
888 10⁸ infectious units per ml) unilaterally into the ARC (n=3). Animals were
889 allowed 6 days for retrograde transport of rabies virus and EGFP expression
890 before perfusion and tissue collection. Sites of afferent input to ARC^{AgRP} neurons
891 were assessed by the presence of EnvA-EGFP positive neurons and the slides
892 imaged on an Olympus VS120 slide scanner microscope.

893

894 ***Rabies collateral mapping***¹⁷

895 Three weeks after unilateral injection of AAV8-EFlα-DIO-TVA-mCherry
896 (University of North Carolina Vector Core; titer 1.1 × 10¹² genomes copies per
897 ml) into the DMH of *LepR-ires-Cre* mice, SADΔG-EGFP (EnvA) rabies
898 (Massachusetts General Hospital Vector Core; titer 10⁷ infectious units per ml)
899 was unilaterally injected into the ARC. Animals were allowed 6 days for
900 retrograde transport of rabies virus and EGFP transgene expression before
901 perfusion and tissue collection. Comprehensive examination of SADΔG-EGFP
902 (EnvA) axonal and retrograde transductions were obtained using 10-15 confocal
903 images of DMH^{LepR}→ARC boutons along the neuraxis using a Zeiss LSM-510
904 confocal microscope.

905

906 ***Statistical analysis***

907 Statistical analyses were performed using Origin Pro 8.6 and Prism 6.0
908 (GraphPad) software. Details of statistical tests employed can be found in the
909 relevant figure legends and supplementary methods checklist. Power analyses
910 were calculated to estimate sample size using statistical conventions for 80%
911 power, assuming a standard deviation of change of 1.0, a difference between the
912 means of 1.5-fold and alpha level of 0.05. In all statistical tests normal
913 distribution and equal variance was established. The data presented met the
914 assumptions of the statistical test employed. No randomisation of animals was
915 conducted since all behavioral tests were within-subject comparisons. Exclusion
916 criteria for experimental animals were a) sickness or death during the testing
917 period or b) if histological validation of the injection site demonstrated an
918 absence of reporter gene expression. These criteria were established prior to
919 data collection. N-numbers represent final number of healthy/validated animals.

920

921 **Data availability**

922 The data that support the findings of this study are available from the
923 corresponding author upon request.

924

925 **References:**

926

927 30. Leshan, R.L., Bjornholm, M., Munzberg, H. & Myers, M.G., Jr. Leptin
928 receptor signaling and action in the central nervous system. *Obesity (Silver*
929 *Spring)* **14 Suppl 5**, 208S-212S (2006).

930 31. Parton, L.E., *et al.* Glucose sensing by POMC neurons regulates glucose
931 homeostasis and is impaired in obesity. *Nature* **449**, 228-232 (2007).

932 32. Garfield, A.S., *et al.* A neural basis for melanocortin-4 receptor-regulated
933 appetite. *Nat Neurosci* **18**, 863-871 (2015).

934 33. Picelli, S., *et al.* Full-length RNA-seq from single cells using Smart-seq2.
935 *Nat Protoc* **9**, 171-181 (2014).

936 34. Petreanu, L., Huber, D., Sobczyk, A. & Svoboda, K. Channelrhodopsin-2-
937 assisted circuit mapping of long-range callosal projections. *Nat Neurosci* **10**, 663-
938 668 (2007).

939 35. Atasoy, D., Aponte, Y., Su, H.H. & Sternson, S.M. A FLEX switch targets
940 Channelrhodopsin-2 to multiple cell types for imaging and long-range circuit
941 mapping. *J Neurosci* **28**, 7025-7030 (2008).

942 36. Franklin, B.J.a.P., G. *The Mouse Brain in Stereotaxic Coordinates* (Academic
943 Press, Elsevier, New York, NY, 2008).

944

945

Figure 1

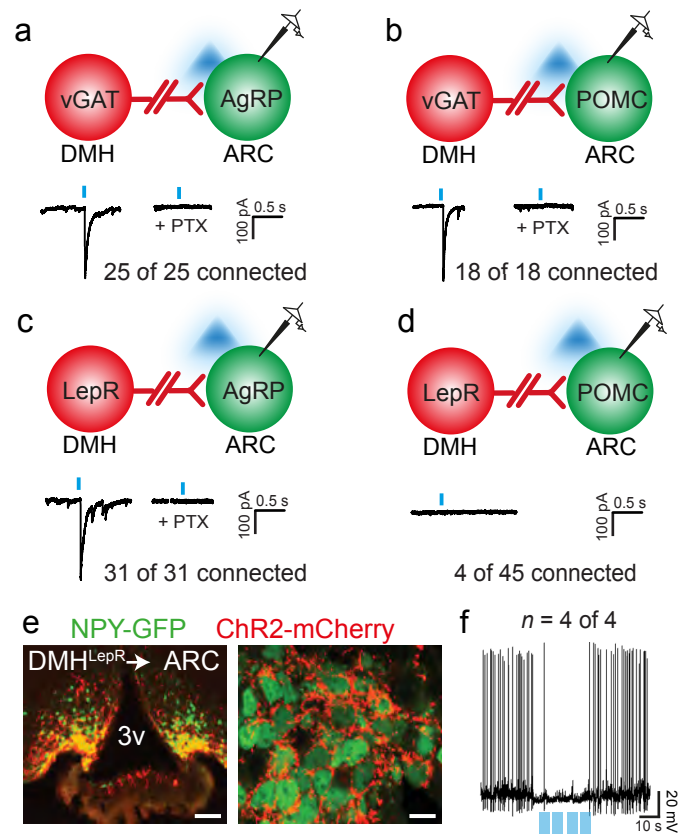


Figure 2

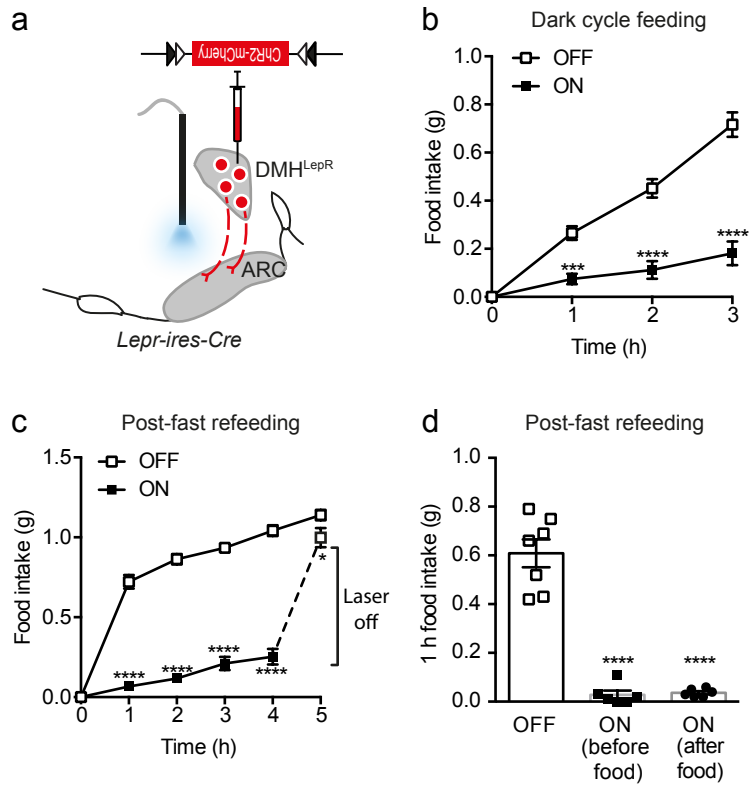


Figure 3

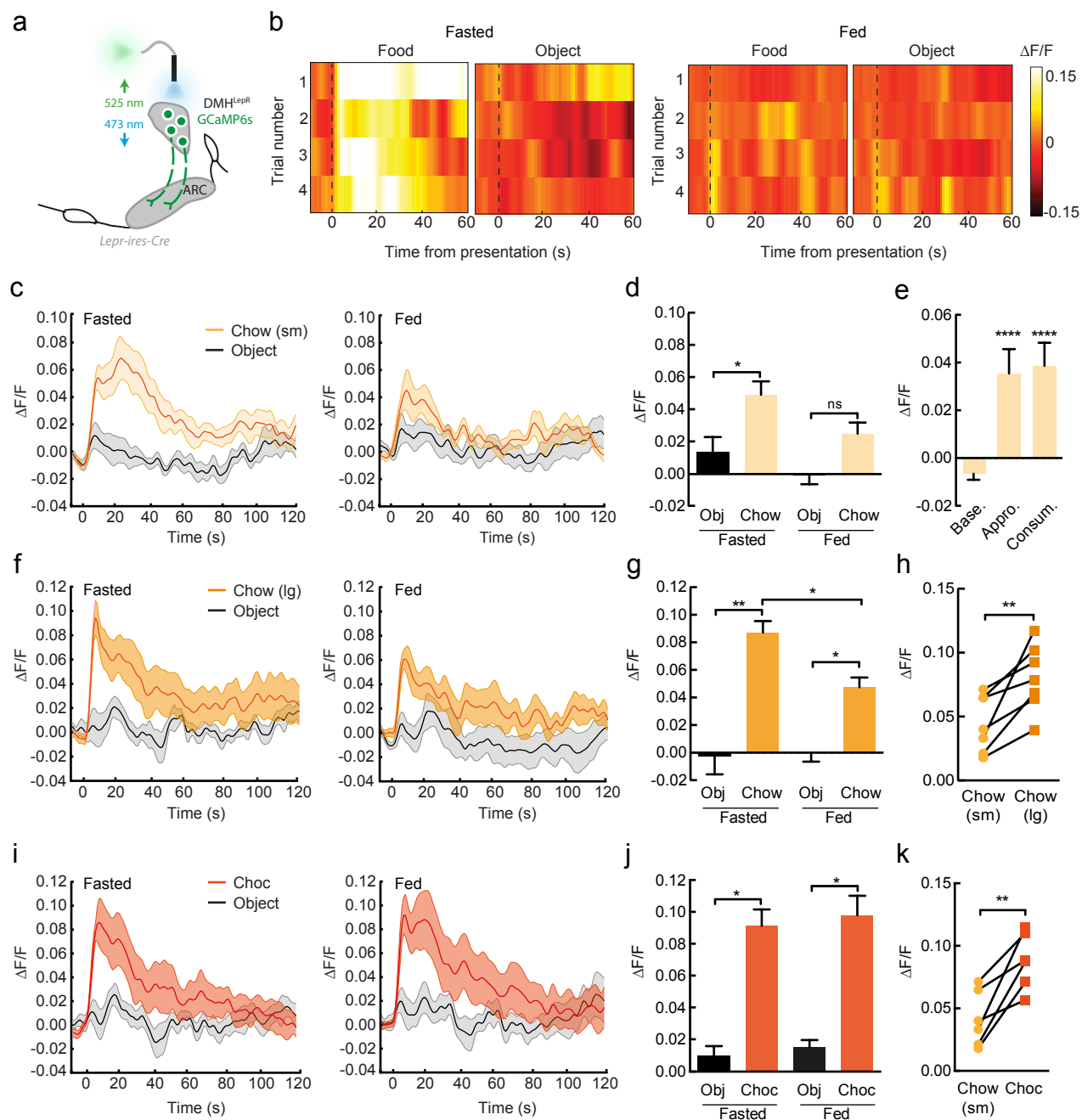


Figure 4

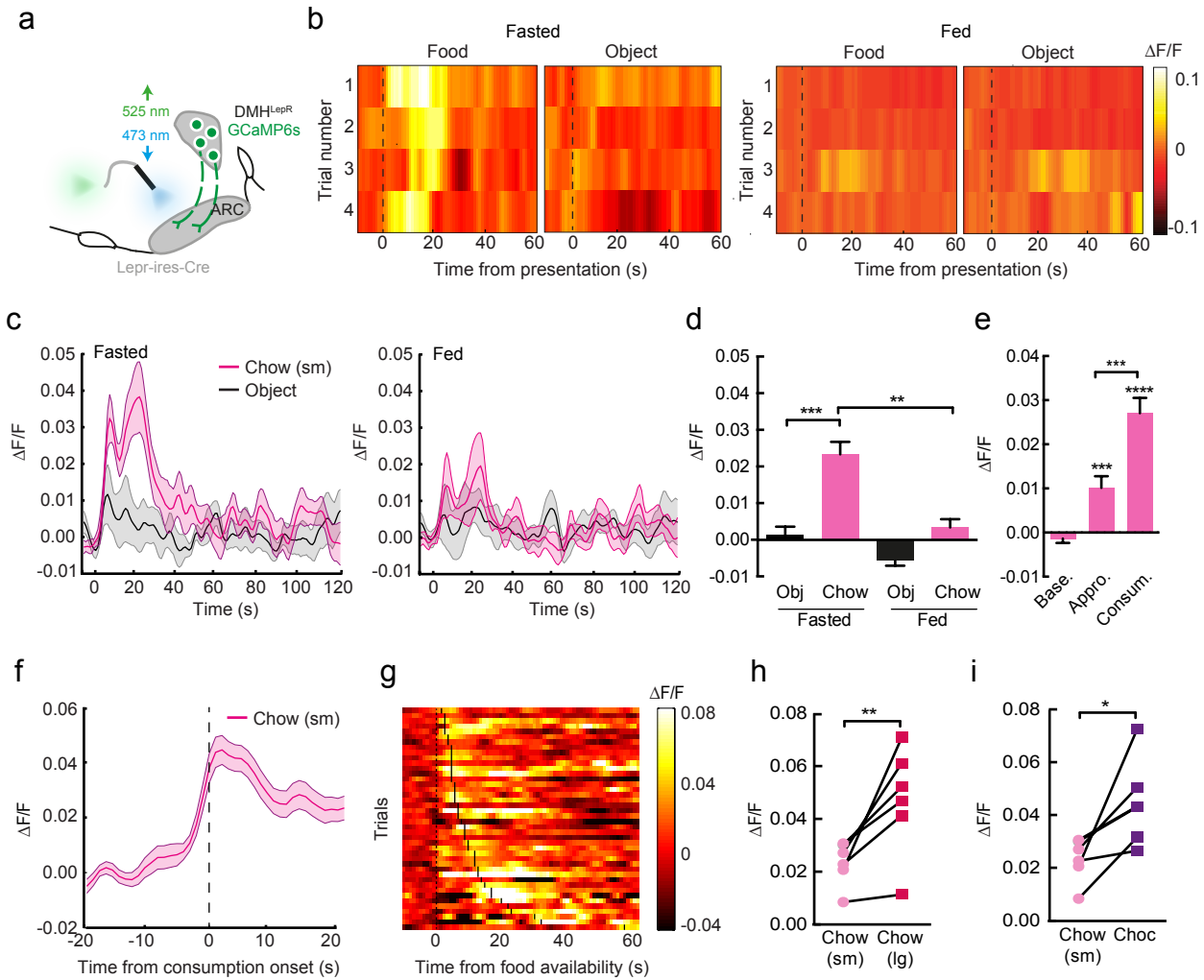
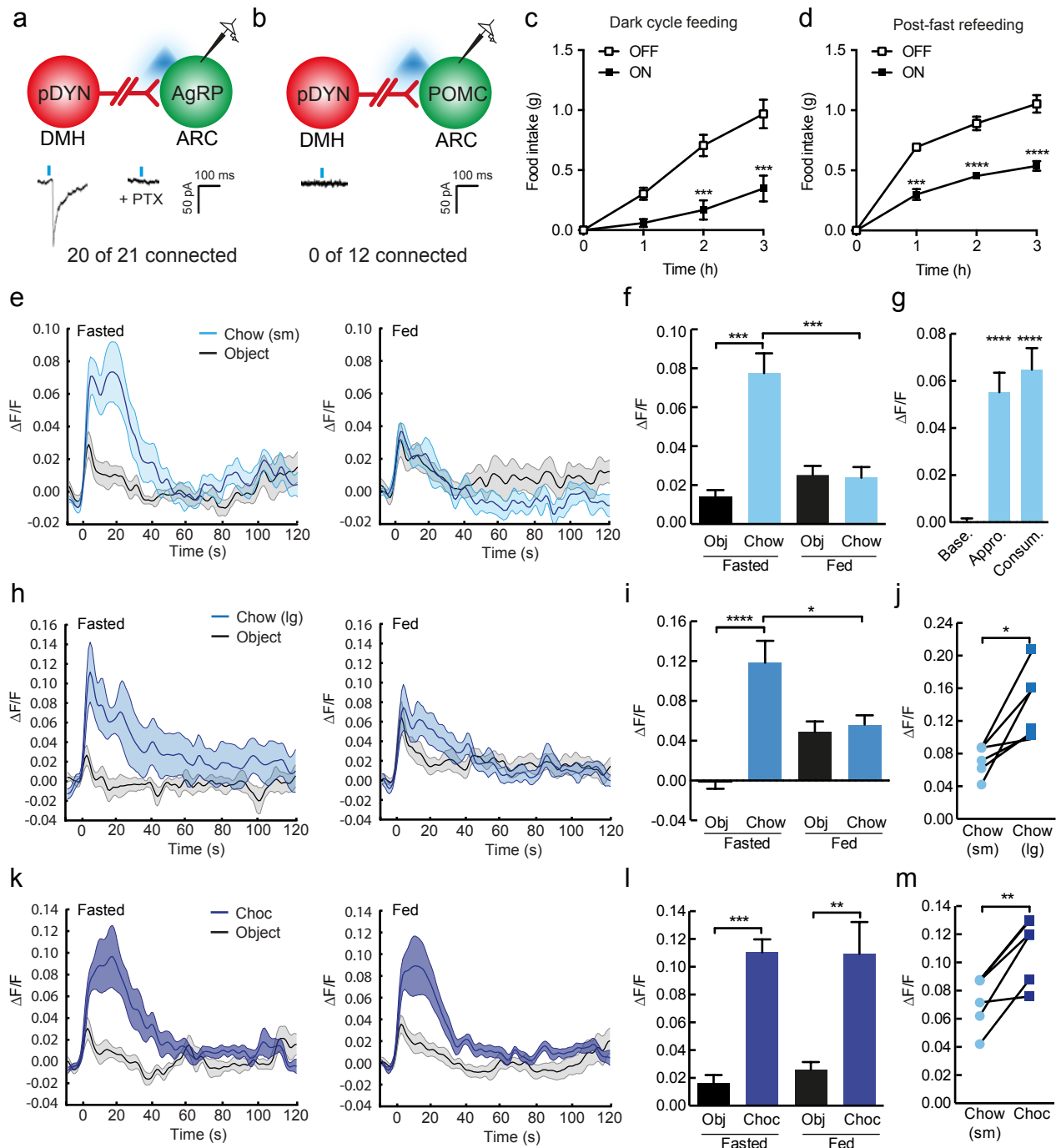
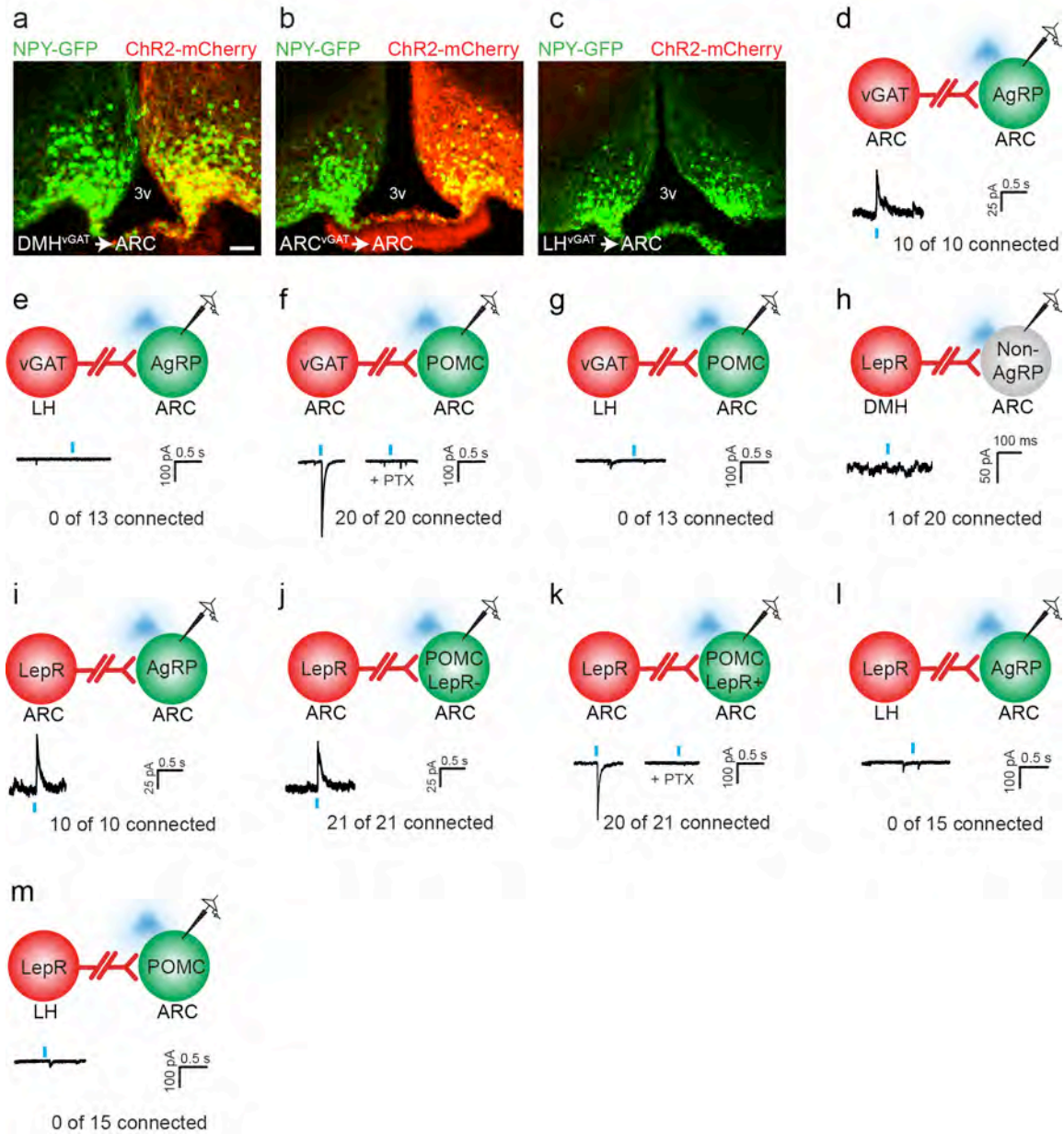


Figure 5

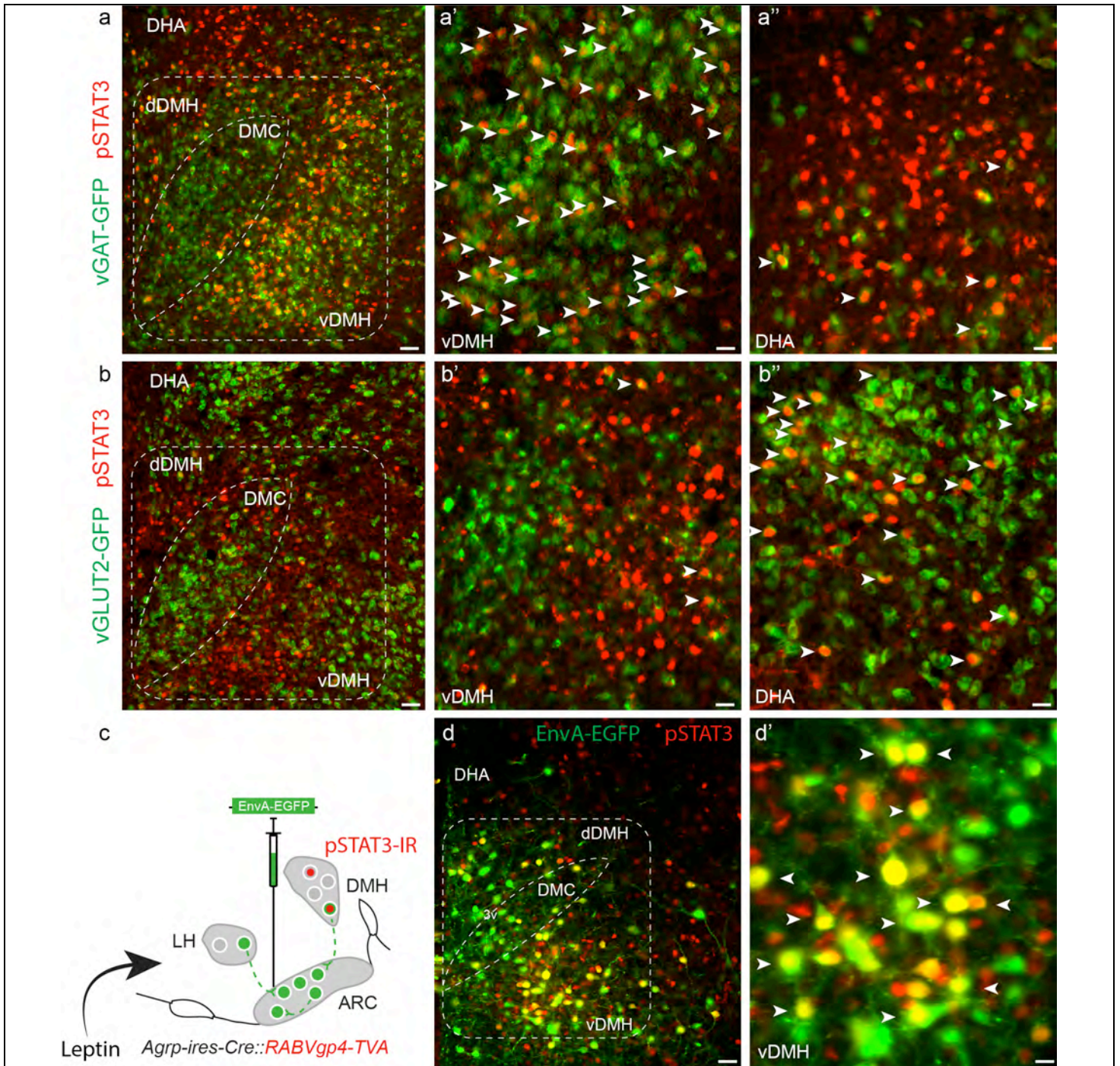




Supplementary Figure 1

Analysis of GABAergic afferents to ARC^{AgRP} and ARC^{POMC} neurons

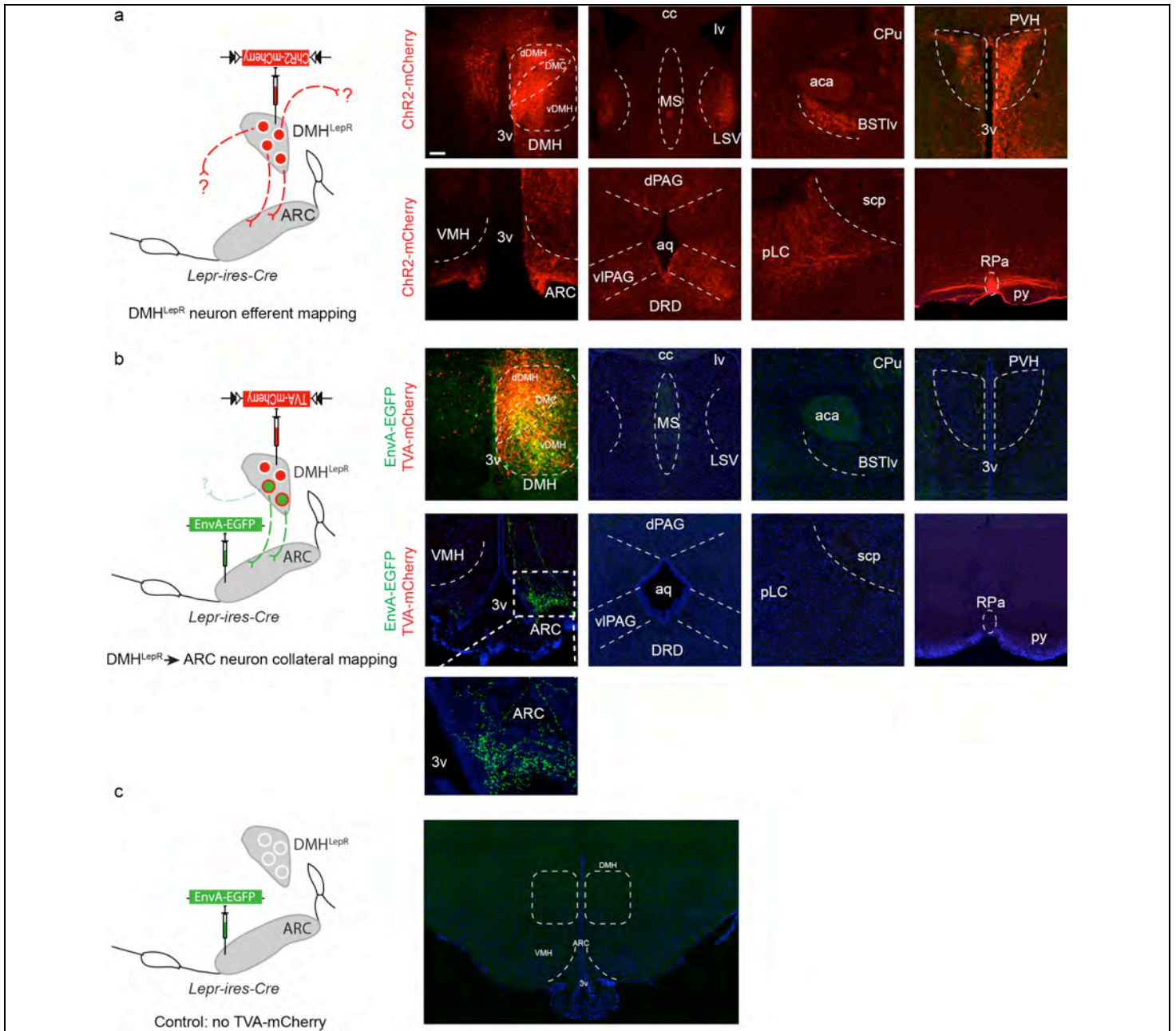
a-c, ARC-projecting vGAT afferents arising from DMH, ARC and LH. **d-l**, CRACM analysis of monosynaptic afferents from vGAT- or LepR-expressing neurons in the ARC and LH. **d-e**, 100% of recorded ARC^{AgRP} neurons receive GABAergic input from local ARC^{vGAT} neurons (d) but not distal LH^{vGAT} neurons (e). **f-g**, 100% of recorded ARC^{POMC} neurons receive GABAergic input from local ARC^{vGAT} neurons (f) but not distal LH^{vGAT} neurons (g). **h**, DMH^{LepR}→ARC neurons do not engage non-AgRP neurons. **i-m**, 100% recorded ARC^{AgRP} (i) and ARC^{POMC} neurons (j-k) receive GABAergic input from local ARC^{LepR} neurons but not LH^{LepR} neurons (l-m). Abbreviations, 3v, third ventricle; PTX, picrotoxin. Scale bar in a, 100 μm and applies to all images.



Supplementary Figure 2

GABAergic DMH^{Lepr^K} neurons are localized to the ventral DMH

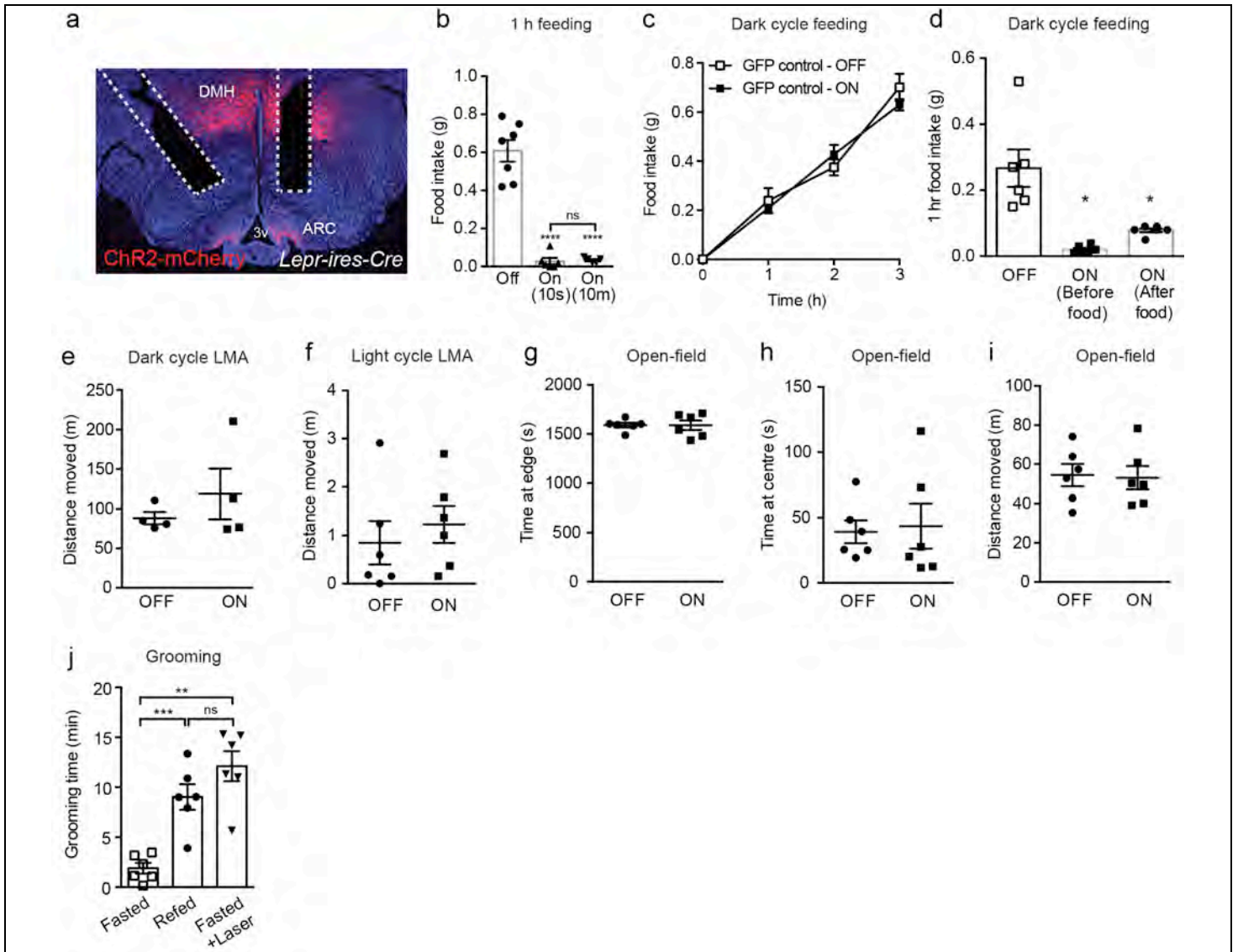
a, GABAergic (vGAT-expressing; green) leptin responsive DMH neurons, as demarked by pSTAT3-immunoreactivity (red), are predominantly localized to the ventral DMH. **b**, glutamatergic (vGLUT2-expressing; green) pSTAT3-immunoreactive (red) neurons are predominantly localized to the dorsal hypothalamic area (DHA) and dorsal DMH. **c**, leptin responsive EnvA-EGFP-labeled ARC^{AgRP} afferents within the DMH are localized to the ventral DMH. White arrows denote GFP and pSTAT3 colocalization. Abbreviations, dDMH, dorsal DMH; DHA, dorsal hypothalamic area; DMC, DMH central part; vDMH, ventral DMH. Scale bar in **a**, **b** and **d**, 100 μ m; in **a'**, **a''**, **b'** and **b''**, 50 μ m; in **d'**, 30 μ m. Each experiment was reproduced in 2-3 mice.



Supplementary Figure 3

DMH^{Lepr} → ARC neurons do not collateralise to other efferent sites

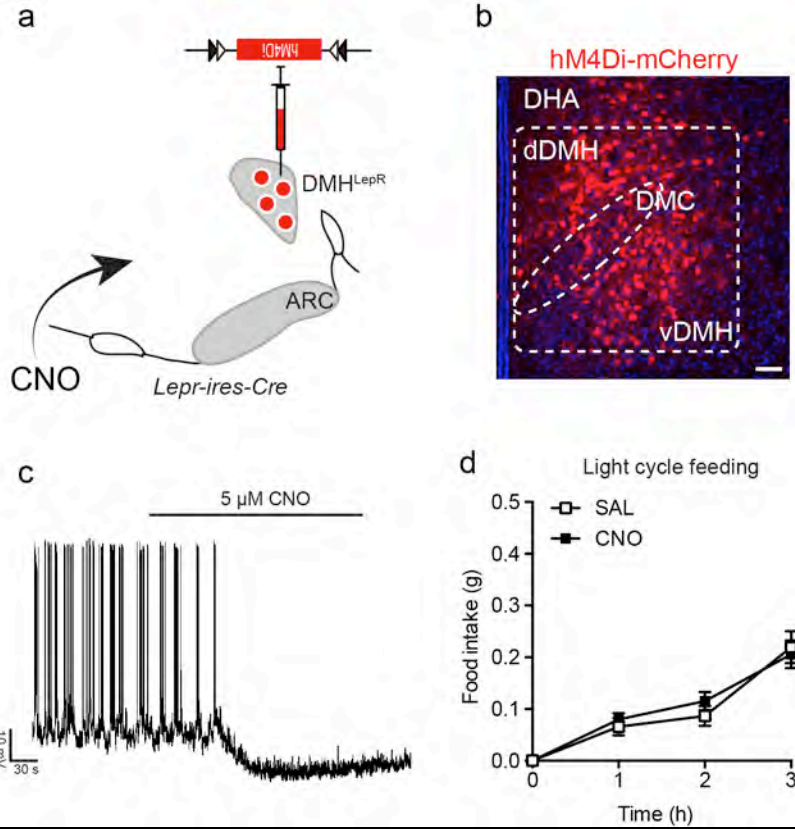
a, histological sections throughout the rostral-caudal extent of the mouse brain demonstrating the efferent projections of DMH^{Lepr} neurons (labelled with ChR2-mCherry) to the lateral septum, ventral part (LSV); bed nucleus of the stria terminalis, lateroventral part; paraventricular nucleus of the hypothalamus (PVH); arcuate nucleus (ARC); ventrolateral periaqueductal grey (VIPAG); pre-locus coeruleus (pLC) and raphe pallidus (RPa). **b**, Rabies collateral mapping suggests that DMH^{Lepr} → ARC neurons do not collateralise to any efferent sites. **c**, in the absence of the TVA-mCherry helper virus no EnvA-GFP infectivity is observed, demonstrating the necessity of TVA for cellular entry of the EnvA virus. Abbreviations, 3v, third ventricle; aca, anterior commissure, anterior part; aq, aqueduct; cc, corpus colosum; CPu, caudate putamen; dPAG, dorsal periaqueductal grey; DRD, dorsal raphe nucleus, dorsal part; py, pyramidal tract; scp, superior cerebellar peduncle; VMH, ventromedial nucleus of the hypothalamus. Scale bar 100 μ m and applies to all images. Each experiment was reproduced in 2-3 mice.



Supplementary Figure 4

Optogenetic stimulation of DMH^{LepR}→ARC terminals does not affect general locomotor behavior

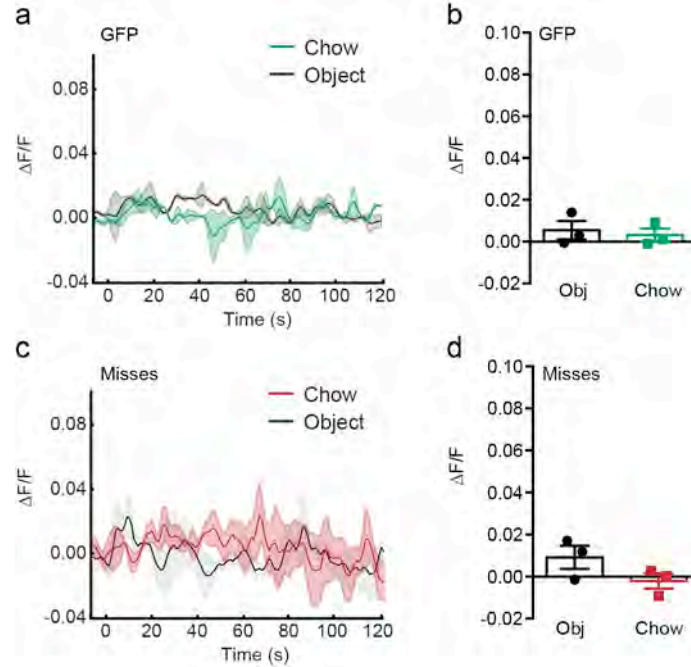
a, representative histological image of bilateral optical fiber placement for photostimulation of DMH^{LepR}→ARC terminals. **b**, photostimulation of ChR2-mCherry expressing DMH^{LepR}→ARC terminals 10 seconds or 10 minutes prior to food presentation reduced food consumption to the same extent, compared to laser off condition (n=6-8; one way ANOVA, $F_{(2,15)}=72.89$, $p<0.0001$; post-doc: OFF v ON (10 s), ****p<0.0001; OFF v ON (10 m), ****p<0.0001; ON (10 s) v ON (10 m), $p=0.94$). **c**, photostimulation of DMH^{LepR}→ARC terminals in the absence of ChR2-mCherry (transduced with cre-dependent GFP) does not influence dark cycle food intake (n=4; repeated measures ANOVA, main effect of treatment and interaction, not significant, main effect of time ($F_{(3,12)}=84.95$, $p<0.0001$). **d**, photostimulation of DMH^{LepR}→ARC terminals in a dark cycle paradigm was sufficient to inhibit food intake when applied before or after food consumption had begun (n=6, repeated measures ANOVA, $F_{(5,10)}=15.52$, $p=0.011$; post-hoc compared to 'OFF': ON (Before), *p=0.02; ON (After), *p=0.03). **e-f**, photostimulation of DMH^{LepR}→ARC terminals does not significantly affect homecage locomotor activity in during a 3 hour dark cycle paradigm (**e**; n=4, paired t-test, $t_{(3)}=0.88$, $p=0.44$) or 1 hour light cycle paradigm (**f**; n=6, paired t-test, $t_{(5)}=0.59$, $p=0.60$) of food. **g-i**, photostimulation of DMH^{LepR}→ARC terminals does not significantly affect the time spent at the edge (**g**; n=6, paired t-test, $t_{(5)}=0.03$, $p=0.97$), the center (**g**; paired t-test, $t_{(5)}=0.19$, $p=0.85$) or the total distance travelled (**h**; paired t-test, $t_{(5)}=0.34$, $p=0.74$) in a novel open-field arena. **j**, photostimulation of DMH^{LepR}→ARC terminals significantly increased grooming to a level comparable to that seen following food consumption (n=6, repeated measures ANOVA, $F_{(5,10)}=23.51$, $p=0.0015$; post-hoc: Fasted v Refed, ***p=0.0009; Fasted v Fasted+laser, **p=0.004; Refed v Fasted+laser, $p=0.31$). All data presented as mean±SEM. Abbreviations, 3v, third ventricle.



Supplementary Figure 5

DMH^{LepR} → ARC neurons are not necessary for the maintenance of satiety

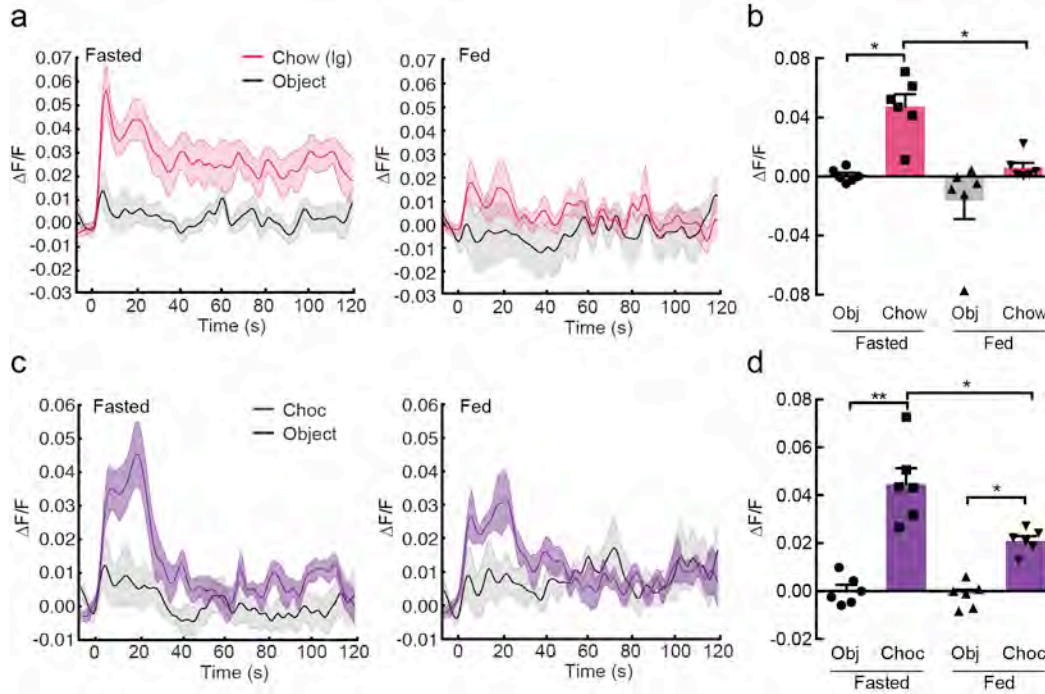
a-b, DMH^{LepR} neurons were transduced with cre-dependent inhibitory DREADD (hM4Di-mCherry). **c**, membrane potential and firing rate of *LepR-ires-Cre::hM4Di-mCherry*^{DMH} neurons decreased upon application of 5 μM CNO during electrophysiological current clamp recordings from acute slices. **d**, chemogenetic inhibition of DMH^{LepR} neurons does not effect light-cycle food intake (n=7; repeated measures ANOVA, main effect of treatment and interaction, not significant, main effect of time ($F_{(3,24)}=43.61$, $p<0.0001$). All data presented as mean±SEM. Scale bar in **b**, 100 μm.



Supplementary Figure 6

Calcium responses in DMH^{LepR} neurons are specific to food presentation

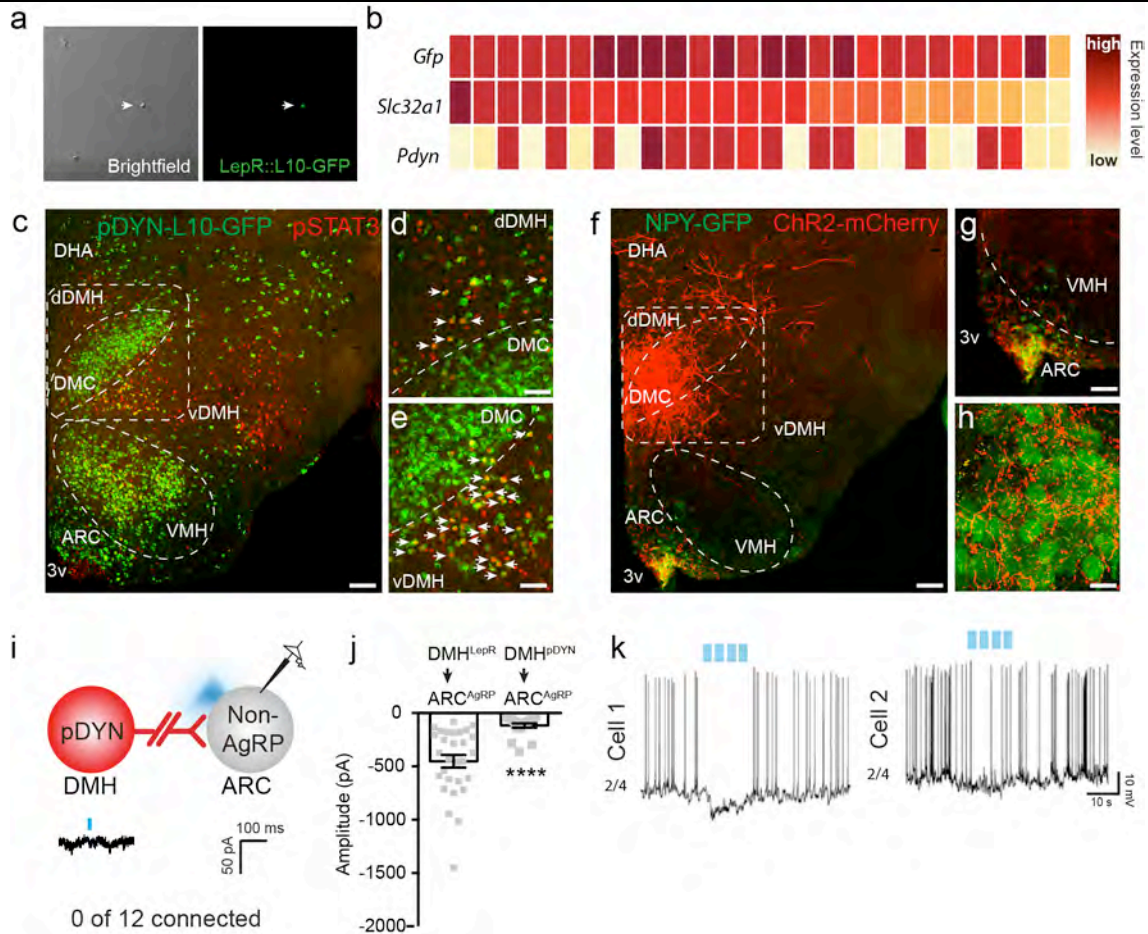
a-b, neither food nor object presentation elicited changes *in vivo* fluorescence in mice with Cre-dependent expression of AAV-DIO-GFP in DMH^{LepR} neurons (a, mean effects from all mice across time, n=3; b, mean response from 0-10s post food presentation, paired t-test, $t_{(2)}=0.41$, $p=0.71$). **c-d**, mice with validated 'misses' in which cre-dependent GCaMP6s was expressed predominantly in the ventromedial nucleus of the hypothalamus LepR-expressing neurons exhibited spontaneous calcium transients but no response to food presentation, compared to a non-food item (c, mean response across all mice across time, n=3; d, mean response from 0-10s post food presentation, paired t-test, $t_{(2)}=1.43$, $p=0.29$). All data presented as mean \pm SEM.



Supplementary Figure 7

DMH^{LepR}→ARC axons respond to food quality

a-b, DMH^{LepR}→ARC axons were rapidly activated upon presentation of a large chow pellet, compared to a non-food object, in an energy-state dependent manner (a, mean effects from all mice across time, n=6; b, mean response from 0-10s post food presentation, repeated measures ANOVA, $F_{(5,15)}=12.71$, $p=0.0033$; post-hoc: Fasted - Obj v Chow, $**p=0.012$; Fed - Obj v Chow, $p=0.335$; Fasted chow v fed chow, $*p=0.02$). **c-d**, presentation of chocolate activated DMH^{LepR}→ARC axons, compared to a non-food object, in both the food restricted and *ad libitum* fed state (c, mean effects from all mice across time, n=6; d, mean response from 0-10s post food presentation, repeated measures ANOVA, $F_{(4,12)}=27.23$, $p=0.0007$; post-hoc: Fasted - Obj v Choc, $**p=0.008$; Fed - Obj v Choc, $*p=0.04$; Fasted choc v Fed choc, $*p=0.04$). All data presented as mean±SEM.



Supplementary Figure 8

DMH^{pDYN} neurons are a subset of GABAergic DMH^{LepR}→ARC neurons

a-b, Single cell picking (a) and quantitative PCR (b) of 25 genetically labeled DMH^{LepR} neurons revealed that a subset of GABAergic DMH^{LepR} neurons express pDYN (14/25). **c-e**, DMH^{pDYN} neurons, demarked by a *pDYN-ires-Cre::L10-GFP* mouse line, in the ventral DMH (green) are leptin responsive, as evinced by pSTAT3-immunoreactivity (red); (white arrows denote GFP and pSTAT3 colocalization). **f-h** DMH^{pDYN} neurons project to the arcuate nucleus of the hypothalamus and innervate ARC^{AgRP} neurons. **i**, DMH^{pDYN} neurons do not make monosynaptic connections with ARC^{non-AgRP} neurons (0/12 connected). **j**, the amplitude of DMH^{pDYN}→ARC^{AgRP} light-evoked IPSCs is significantly smaller than DMH^{LepR}→ARC^{AgRP} light-evoked IPSCs (n=20-29, two-tailed t-test, $t(47)=4.55$, $p<0.0001$). **k**, photosimulation of DMH^{pDYN}→ARC terminals was sufficient to inhibit ARC^{AgRP} action potential firing in some (representative *cell 1*, 2/4 neurons), but not all, ARC^{AgRP} neurons (representative *cell 2*, 2/4 neurons). All data presented as mean±SEM, **** $p<0.0001$. Abbreviations, ARC, arcuate nucleus of the hypothalamus; dDMH, dorsal DMH; DHA, dorsal hypothalamic area; DMC, DMH central part; vDMH, ventral DMH; PTX, picrotoxin. Scale bar in c and f, 200 μ m; in d, e, g, 100 μ m and in h 20 μ m.